Validation of muscle relaxation measurements

van Steen, Marco H.A.

Award date:
1998

Eindhoven University of Technology
Faculty of Electrical Engineering
Department of Measurement and Control
Section Medical Electrical Engineering

Validation of muscle relaxation measurements

M.H.A. van Steen

Thesis for the degree of Master in Electrical Engineering,
Completed in the period May 1997 through March 1998.
Project assigned by: Prof. dr. ir. P.P.J. van den Bosch
Supervisor: Dr. ir. J.A. Blom
In cooperation with: Dr. H.H.M. Korsten, Catharina Ziekenhuis Eindhoven

Abstract

The administration of neuromuscular blocking agents during surgery is directed to suppressing involuntary muscle movements in anaesthetised patients. Muscle relaxants are conventionally administered by bolus injections. This results in a failure to maintain steady relaxation levels. Continuous infusion of muscle relaxants leads to a more stable level of muscle relaxation. The work in this paper is aimed at the optimization of an existing measurement system, and on validation of measurements of muscle relaxation in order to develop in a later stadium a closed-loop feedback controller for muscle relaxation.

An improved version of the data acquisition part of the measurement system was developed. A new digital to analog conversion board was adapted to, interfacing to an integrated anaesthesia monitor was established, and software was developed to collect, present and store the muscle relaxation measurements. The measurement method used in this work is the train-of-four (TOF) method with EMG sensors.

The purpose of the validation algorithm is to detect measurements that are disturbed by artefacts. If the quality of a measurement is doubted, the algorithm should consider it invalid. The final goal is first to discard all measurements that contain artefacts, and secondly to avoid the discarding of valid measurements.

Since there is very little knowledge about the 'correct' shape of the signals, knowledge was acquired by analyzing many parameters of the EMG signals.

The 'heuristic' approach to validation, used in this work, may be summarized as follows:

1. A learning set and a test set of measurements were inspected by eye. In this way, a 'golden standard' was determined for the validation algorithm, and insight in signal properties and artefacts was gained.
2. A large number of parameters was chosen that are based on a single ECAP (evoked compound action potential), on the rate of change between the ECAPs of one TOF, or on the rate of change between TOFs.
3. The parameters were calculated for every measurement in the learning set. The results were presented in histograms.
4. Suitable bounds for the parameters were determined.
5. The criteria were applied to the learning set and the results were compared to the visual inspection.
6. The algorithm was verified with a test set of measurements that is independent of the learning set.
7. If necessary, the algorithm should be optimized by repeating steps 2 through 6 until the results are satisfactory. To assure the independency of the test set, a new test set should be acquired and used in the iteration.

Steps 1 through 6 were carried out. Without the optimization step, the algorithm was able to detect circa 85% of all artefacts. A large number of measurements was incorrectly considered invalid and this number was just on the limits posed by the controller's needs in the steady state phase, and below the demands during the onset phase.
Ways to optimize the algorithm are re-evaluation of the visual inspection, finding parameters that are still more independent of the level of muscle relaxation and tuning the threshold values.

Voorwoord

Vanaf deze plaats wil ik graag al degenen bedanken die op welke manier dan ook hebben meegewerkt aan het afstudeerwerk dat in deze scriptie wordt beschreven.

Ten eerste dank ik dr. Erik Korsten voor het mogelijk maken van de metingen in het Catharina Ziekenhuis, voor zijn enthousiasme en de niet aflatende stroom ideeën. De anesthesie assistenten toonden interesse en een waardevolle kritische blik tijdens de operaties. Frans de Kok van de medisch fysische instrumentatie dienst werkte mee aan het praktische gereedmaken van het meetsysteem.

Verder dank ik Hans Blom voor de goede begeleiding en ideeën, en ook alle andere medewerkers van de sectie E.M.E. voor de praktische ondersteuning en vooral de prettige sfeer.

Ron van der Zwaluw van de firma Datex Medical Electronics was behulpzaam met het oplossen van een aantal technische vragen.

Tot slot wil ik vrienden, bekenden en bovenal mijn ouders bedanken voor de interesse en grote steun tijdens de afstudeerperiode.

Marco van Steen

Table of contents

1. Introduction

1.1 Backgrounds

In the servo-anaesthesia project of the group of Medical Electrical Engineering (E.M.E.) at Eindhoven University of Technology, research is carried out on the question how computer and information technology may help improve the quality of anaesthesia given to patients in intensive care units and operating theatres.

One of the directions in this program is the development of automatic closed loop control systems that take over routine tasks from the anaesthetist. Such tasks include stabilization of blood pressure and keeping the patient's muscles relaxed to a certain degree. It is tried to develop systems that are suitable for clinical use on a routinely basis.

Benefits of such relatively simple control systems may be various. The desired level of effect will be more constant, and the patient will only receive the amount of drug that is needed for the desired effect. By taking over routinely and time consuming tasks, the anaesthetist may have more attention for the patient, and be more alert to signs of complications.

Earlier, a controller for blood pressure has been developed and implemented succesfully at E.M.E. [Zwart 1992]. Now, research is focusing on a controller for muscle relaxation [Hoevenaren 1992, Scheepers 1992, Smans 1993]. The general architecture of this system is shown in figure 1.1.

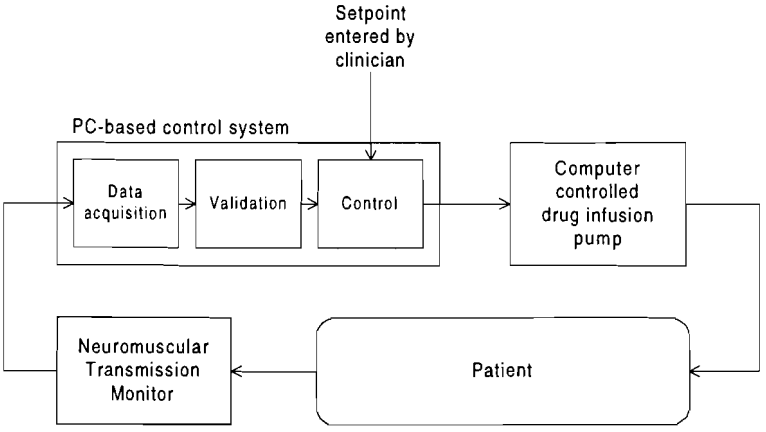

Figure 1.1 - Architecture of a control system for muscle relaxation.

1.2 Control of muscle relaxation

During operations, most patients are given muscle relaxant drug in order to suppress unintended movements that might disturb the surgeon's work. The relaxant makes all skeletal muscles insensitive to nerve action potentials. Since the ventilatory muscles are also paralyzed, these patients are ventilated artificially. The heart and the digestive muscles are not affected.

In normal clinical practice, the desired level of muscle relaxation is reached by injecting an initial dose of relaxant drug in a vein and maintained by smaller repeated injections. This causes large fluctuations, and in most cases an initial overshoot in the level of relaxation. An automatic control system might overcome these problems.

From literature, it is known that existing control systems for muscle relaxation may show good performance in terms of deviation from the target level, but often show problems concerning the measurement system [Olkkola 1996]. As a solution, some focus on robust control algorithms, while others even used two measurement systems in parallel to increase the reliability [Mason 1997]. No reports on attempts to automatically validate the muscle relaxation measurements have been found in literature. It is also unclear how the control systems react in case of heavily disturbed measurements, and if safe behaviour can also be guaranteed in these situations.

The major causes of problems in case of NMT monitoring by EMG are:
- incorrect positioning of the stimulating and recording electrodes,
- unintended direct stimulation of the muscle (via the skin surface instead of via the nerve),
- electrical activity in parts of the muscle that move, but don't contract,
- diathermia (use of an electric knife),
- movements,
- electrode cables getting loose.

The influence of these artefacts on the final controller performance may be reduced in several ways: for example by preventing their occurence, by automatic checking of the signal quality (validation), and by designing a control algorithm that is robust to noise at its sensor input.

At E.M.E., work has been done on the first possibility. E.g. an optimal electrode positioning for reliable monitoring was determined [Smans 1996]. This may prevent failing calibration procedures and direct stimulation. Careful shielding and grounding of cables and equipment may reduce the influence of diathermia. Signal processing, especially low-pass filtering, may also reduce spikes caused by diathermia. Loose electrode cables are signalized by the NMT-monitor itself, but do lead to incorrect measurement values.
But since it is still possible that measurements are disturbed, each measurement should be validated before use, to make sure that the information supplied to the controller is only correct or missing, but not incorrect. A method to construct a validation algorithm should be developed. This will be discussed in paragraph 1.4.
Finally, although some recommendations about the control system will be included in this report, its actual design is beyond the scope of this work.

1.3 Data acquisition

In previous work at E.M.E., a data-acquisition system for the measurement of muscle relaxation has been set up [Hoevenaren 1992, Smans 1993]. A Relaxograph, type NMT-100, produced by Datex [Datex Relaxograph User's Manual], was used as a measuring device, of which the analog output was connected to a Labmaster data-acquisition PC-board. The PC software was written in Borland Pascal 7.0. A closer look showed that some improvements could and/or should be made:

1. The existing software did function correctly, but its structure could be improved, in order to be able to include the validation and control system parts.

2. Nowadays the Relaxograph has become part of an integrated anaesthesia depth unit (ADU), which is able to monitor the most important physiological patient data, and also contains a ventilation and anaesthetic vapor unit. A number of operating rooms in the Eindhoven Catharina Hospital has been equipped with these AS/3 monitors of Datex-Engström (Finland). Because of their greater flexibility, ease of use, and interfacing possibilities, and because staff had become familiar with this equipment, it would be desireable to interface to these monitors.

3. Hoevenaren and Smans both reported serious problems with the Labmaster board. Interrupts did not function, there was no high-level driver software available, documentation contained errors, and cabling was sensitive to EM interference. Although eventually work-arounds for these problems were found, it was doubted if such hardware was reliable and safe enough for our goal. Moreover, better hardware had become available in the mean time.

These three reasons lead us to the reconstruction of the data acquisition system hardware and software. It will be discussed in chapters 2 and 3.

1.4 Validation of the measurements

As pointed out earlier, the task of a validation algorithm will be, to check if a given measurement is disturbed by artefacts or not.
The basic assumption in this is, that measured EMG-waveforms contain enough information to judge their validity. This assumption seems reasonable because, as was seen in EMG-data previously recorded by Joost Smans, most sources of artefacts cause visible distortions in the EMG-signals. Although the waveform varies greatly between patients and during operations, in general the variation between two successive valid measurements is limited. In case of deep relaxation, when the signal level is low, validation will probably be more difficult, because the signal is noise-like.

So, by qualitative and quantitative analysis of EMG signals, combined with knowledge about the electrophysiology of nerves and muscles, we may gather knowledge about the shape of correct EMG signals. This knowledge may be expressed in simple rules, that can be implemented in a computer program.

The performance of this program should be tested, by comparing it to some 'golden standard'. Since experts on the visual interpretation of muscle relaxation signals are hard to find, I decided to judge the signals by myself.

1.5 Formulation of the project

As pointed out in the above paragraphs, two main goals were identified:
- Develop a real-time measurement system for muscle relaxation: Study the usefulness of the existing software and develop software for a real-time measurement system, which reads in the neuromuscular transmission monitor and presents the muscle relaxation in % to the clinician. Test this measurement system on a number of patients and evaluate reliability and accuracy.
- Develop a method for the design of a validation algorithm, implement such an algorithm and test it on a set of measured signals.

Literature on the above subjects should be studied to identify problems and their possible solutions.

1.6 Contents of this report

The development of a new data-acquisition system is described in chapters 2 and 3. Chapter 2 covers the hardware, and chapter 3 the software.

After that, we will focus on validation methods. Chapter 4 outlines the goals and possible methods for validation. Every validation method makes use of a priori knowledge about the signal. In chapter 5, analyses of TOF signals are described that should result in the needed knowledge. Based on this knowledge, criteria for valid signals are derived.

To test the data acquisition system and to acquire a set of TOF signals to test the validation algorithm, a series of measurements have been carried out in the operating room. Chapter 6 presents an evaluation of both the data acquisition system and the validation algorithm.

Finally, chapter 7 lists conclusions and suggestions. Points of attention for further research will also be presented.

2. Hardware

In this chapter, we will describe the hardware used to measure the level of muscle relaxation. The main questions are: how can the level of muscle relaxation be measured, and how can the data be made available for processing with a PC. The first paragraph tries to answer the first question, while the rest of the chapter is devoted to the second. In the second paragraph, the reasons for developing two versions of the data acquisition system will first be pointed out. After that, the A/D conversion board, that is common to both versions, will be described. Finally, some details of both links will be presented.

2.1 Measurement of muscle relaxation

First of all, it should be noted that this paragraph is only meant as a short introduction to the method of muscle relaxation measurement used in our system. Hoevenaren [Hoevenaren 1992] has investigated the several methods of measurement, and motivated the choice for this method. Smans [Smans 1993] further optimized the method. For the physiological background of neuromuscular block, the reader may refer to [Feldman 1996].

The level of muscle relaxation can be measured by a neuromuscular transmission (NMT) monitor. This monitor applies a pattern of electrical stimuli to a nerve via surface electrodes. Depending on the level of muscle relaxation, more or less muscle fibres of the muscles that are connected to the nerve will contract in response to stimuli. This contraction is then measured by force, movement, acceleration, EMG or other sensors. We chose to use EMG sensors. When placed on the skin near the belly of the muscle, these surface electrodes pick up the superimposed

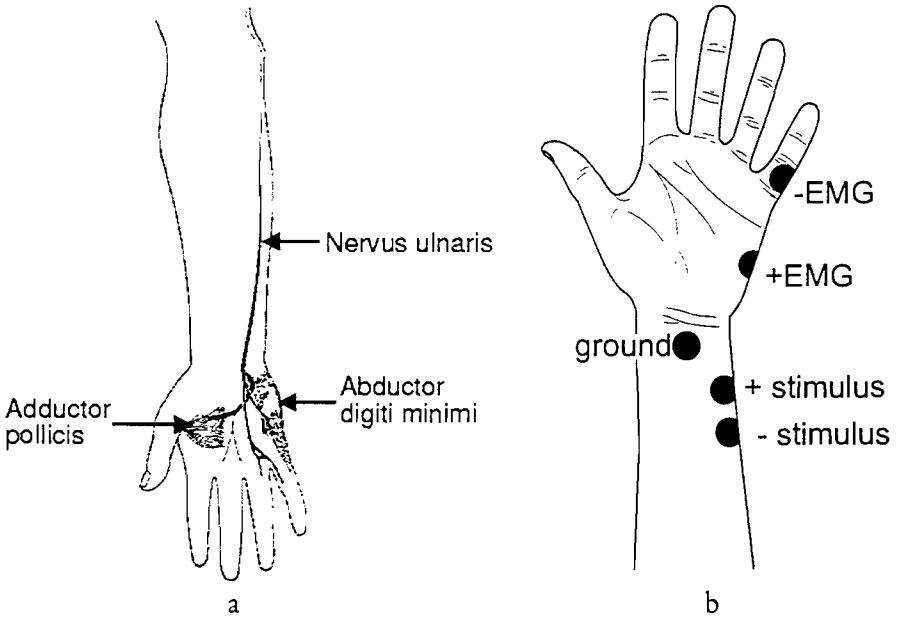

Figure 2.2 - a) position of nervus ulnaris and abductor digiti minimi, b) optimal electrode placement [Smans 1996].

electrical activity of a number of contracting muscle fibres. The measured EMG waveform is often referred to as an evoked compound action potential (ECAP). The pattern of stimuli we used is the so-called train-of-four (TOF) stimulation. This means that four stimuli, each lasting 100 μs,

are applied at 0.5 second intervals. This pattern is repeated every 20 seconds. So every 20 seconds, the NMT-monitor carries out one measurement.
The ulnar nerve (in the forearm) and the abductor digiti minimi (a muscle on the little finger, see figure 2.1a) form a convenient nerve/muscle combination. When this combination is used, electrodes should be placed according to figure 2.1b.

2.1.1 Train-of-four response

The EMG response to TOF stimulation (see figure 2.2) consists of four twitches. At the moment of stimulus, a stimulus artefact is seen. This is caused by conduction over the skin, not by muscle contraction. Since the internal amplifier is gated only after 3 ms, the stimulus artefact is not present in the output signal. After 3 ms, a more or less biphasic potential can be seen, that lasts for circa 25 ms. It is caused by the depolarization front in the muscle tissue that moves under the electrode [Metingen in de geneeskunde I]. Note that the actual movement is a much slower process that lasts hundreds of ms.

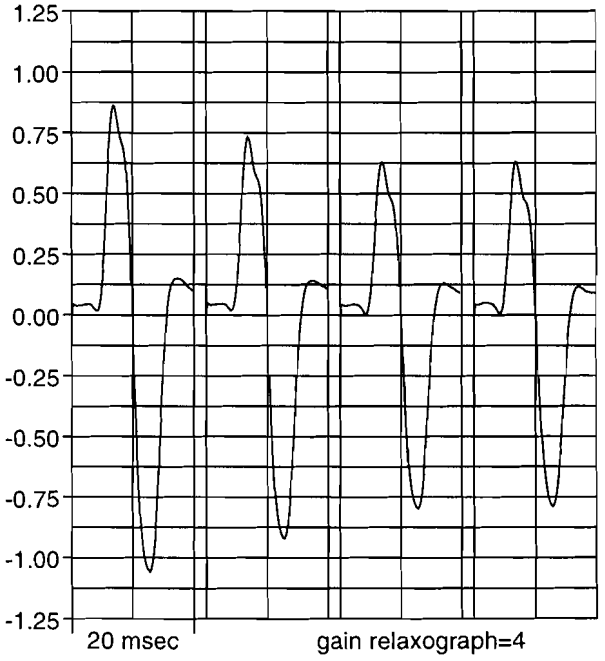

Figure 2.3 - EMG response to train-of-four stimulation measured at the output of the NMT (in V)

2.1.2 Signal processing by the NMT monitor

Since the stimulus artefact and the small, slow afterwave are irrelevant for this purpose, the NMT-monitor uses a time-window from 3 to 18 ms after each stimulus. The signal is amplified circa 1000 times, band-pass filtered (from 60 to 400 Hz), rectified and integrated. The final integrated voltage is proportional to the surface under the curve between 3 and 18 ms. It is referred to as T_n, where n = 1, 2, 3, 4 for the different twitches in a TOF. T_{ref} is the T value in the normal, unrelaxed state.

Two clinically important parameters may be derived from T_1, T_4 and T_{ref} : muscle relaxation and muscle fade.

1. *Muscle relaxation* is defined as 100% - 100% · T_1 / T_{ref}. It can only be calculated if a reference measurement (T_{ref}) has been carried out before injection of muscle relaxant.
2. *Muscle fade* is defined as 100% - 100% · T_4 / T_1. As can be seen in figure 2.2, the fourth twitch of a TOF is markedly smaller than the first. Muscle fade is also called TOF ratio, or TOF value.

One can state that, within certain limits, the fade increases when the muscle relaxation increases. Because of this correlation between the muscle relaxation and muscle fade, the muscle fade is often used as a clinical measure for relaxation. It must be noted though, that the correlation is weak and depends on many factors. When T_1 / T_{ref} is low, T_4 / T_1 becomes unreliable because T_4 is very small and noise-like. The two measures can not be used interchangeably, and the most reliable measure is T_1 / T_{ref}.

The NMT monitor presents T_1 / T_{ref} (if a calibrated measurement was done) as well as T_4 / T_1 on a display screen.

After the electrodes have been placed and the NMT cable has been connected, but before the muscle relaxant drug is administered, the clinician should have the NMT monitor execute an automatic calibration cycle. In this cycle the monitor does the following:
1. It sets the gain of the internal EMG amplifier,
2. It applies a series of stimuli (at 0.5 sec intervals) with increasing current (up to 70 mA) until the EMG response does not increase any further (i.e. all innervated muscle fibres are contracting). By adding 15% to that current, the supramaximal stimulus current is found, that will be applied during the rest of the operation.
3. A few seconds after that, four supramaximal stimuli are applied at 1 sec intervals. The average T-value of the responses is calculated, and used as T_{ref}.

If this calibration fails, the user can try to recalibrate or continue in uncalibrated mode. In this mode only the muscle fade is displayed.

For testing purposes, a Datex EMG train-of-four simulator (property of the Catharina hospital) was used. It is connected to the NMT electrodes, and delivers square pulses of circa 11 ms in response to a stimulus. The output level as well as the muscle fade can be adjusted. By using this simulator, the developer does not need to be connected to the NMT monitor himself.

2.2 Interfacing to Relaxograph and to AS/3 ADU

Since the raw EMG signal is needed for validation purposes, a link between PC and NMT monitor should be set up, that makes this data available in a digital format. For synchronisation purposes, a trigger signal is required to note when the monitor stimulates the patient.

Previously, a Datex Relaxograph NMT-100 was used as a measuring device. As pointed out in paragraph 1.3, new anaesthetic depth units (ADUs) with integrated NMT-monitors had been purchased by the Catharina Hospital. The NMT monitor module of the ADU has several advantages over the older Relaxograph:

- the user interface is much easier: for the NMT module, there is only one button to start the calibration cycle, and one button to start/stop the NMT monitoring,

- not only train-of-four (TOF), but also double burst stimulation (DBS), post tetanic count (PTC) and single twitch stimulation modes are supported, and the stimulus duration can be configured to be 100, 200 or 300 μs,
- as a sensor, either EMG sensors or accelerographic sensors may be used. The accelerographic sensor signal, is however not available at the output, so it is not suitable for our purpose,
- the ADU stores all collected physiological data (also the NMT data). The ADU can show these trends on a display or print them.
- almost all measured physiological signals (ECG, blood pressure, oxygen saturation, ventilatory flows, -pressures and -concentrations, administered anaesthetic vapors etc.) are available on the digital or analog outputs. So, if the muscle relaxation control algorithm might also need other data it can use the same physical link.

Disadvantages are that the digital serial interface is more complex than the Relaxograph's serial link, and that the ADUs are in permanent use in the operating rooms, so the time to test the PC-ADU interface is limited.

A 'Relaxograph' that was no longer in use could be borrowed from the hospital, so it was decided to make interfaces to the Relaxograph as well as to the new monitors. In case the latter interface would not function well enough, the former could be used as a back-up.

2.3 A/D conversion board

2.3.1 Selection of a data acquisition board

To digitize the analog EMG signals, an A/D conversion board is used. Because of the problems previously experienced with the Labmaster A/D board [Smans 1993], a new board was selected.
The main demands to a suitable board, together with two alternatives to the Labmaster are presented in table 2.1.
We need one input channel for the EMG signal, and one for a trigger signal. The output voltage range of the Relaxograph and the ADU are -10...+10 V and -5...+5 V, respectively. So the input voltage range of the board should at least be -10...+10 V.

Table 2.1 - Demands to a data-acquisition board and the performance of two existing comparable boards

Feature	Required	Keithley Metrabyte DAS 1402 and Advantech PCL818L
Number of analog input channels	2 (differential)	8 (differential)
(differential, single-ended mode)	2 (single-ended)	16 (single-ended)
Number of digital input channels	0	4*
Number of digital output channels	0	4*
Maximum input voltage range	-10 to +10V	-10 to +10 V
Programmable gain	yes	yes: 1, 2, 4, 8 times
Sample frequency	> 600 Hz	up to 100 kS/s
Device driver software supports	DOS / Pascal	DOS, Windows, C, Pascal, Visual Basic
Data transfer mode	DMA	DMA, I/O, interrupt
Resolution (bits)	> 8	12

*) Advantech board has 16 digital inputs and 16 digital outputs

Since the EMG signal contains almost no frequencies above 150 Hz, the sample frequency of the A/D board should be higher than 300 Hz. As a margin of safety, the required sample frequency should be at least 600 Hz.

The EMG signal should be digitized with a good accuracy. Since the amplitude of the EMG signals may decrease a factor 100 or more, quantization errors should be kept to a minimum. This can be done by increasing the A/D board gain for small signals, and by choosing a board with a high resolution A/D converter (more than 8 bits).

The performance of two selected boards was very similar, and sufficient for our purpose. Because of practical reasons the Keithley Metrabyte DAS 1402 board was selected eventually. With the board comes a driver library that can be linked with Pascal, C and Basic programs.

2.3.2 Characteristics of the DAS 1402 board

Now we will briefly discuss how the board acquires, converts and stores samples of the analog input signals. The four digital inputs and four digital outputs of the DAS 1402 board are not covered here.

The analog signals to be measured are connected to one or more of the 16 physical input channels on the board's I/O connector. The inputs may be operated in *differential* mode or in *single-ended* mode. In differential mode, the difference between two physical inputs is measured and mapped to a logical channel. In single-ended mode the voltage between an input and ground is measured. In differential mode there are 8 analog input channels available while in single-ended mode there are 16 channels. The mode is set by a dip switch on the A/D board.

The inputs may be configured for *unipolar* or *bipolar* voltages, with an other dip switch. Unipolar voltages should always be equal to or greater than 0V, while bipolar voltages may have positive and negative values. We selected bipolar voltage mode because the Relaxograph's output range is -10..+10V.

The incoming analog signal is amplified by an amplifier with programmable gain. For the DAS1402 board, this gain can be set to 1, 2, 4 and 8 times. By increasing the gain for small signals, the 4096 steps of the 12 bit A/D converter are used for a smaller input voltage range. In this way, the resolution can be improved. The relationship between gain and resolution is given in table 2.2. The gain-code is a number, supplied to the driver software to set a given gain factor.

Table 2.2 - The relationship between gain, gain code, input voltage range and resolution of the 12 bit A/D converter

Gain	Gain code	Input voltage range	Resolution
1	0	-10 V to 9.995 V	4.88 mV
2	1	-5 V to 4.9976 V	2.44 mV
4	2	-2.5 V to 2.4988 V	1.22 mV
8	3	-1.25 V to 1.2494 V	0.61 mV

When using multiple channels, these should be connected to successively numbered input channels. The first and last channel in a scan can be set via software. Since there is only one A/D converter (ADC) present, only one channel may be sampled at the same time. To sample multiple channels, a multiplexer connects them to the ADC one after another.
The scanning of the channels to sample can be done in two modes, that can be set by software. In *'paced mode'*, the sampling of the channels is done at regular intervals. After finishing a scan, the next scan is started after such an interval. In *'burst mode'* the ADC samples the channels one after another at very short intervals, and then waits until the next scan should be performed. In this mode, the channels can be sampled at 10 µs intervals.

Acquisition is always initiated on command of the PC. There is no provision for a hardware trigger that initiates the conversion without intervention of a software routine.

Each sample is stored in memory as a 16 bit word. The digitized data (called a 'count' value) are stored in the highest 12 bits, while the channel number is stored in the lower four bits. The lowest voltage in the input voltage range corresponds to a count value of 000h, while the highest voltage corresponds to FFFh. Therefore, to calculate the voltage V, corresponding to a given 16 bit word W, the following formula should be applied:

$$V = (([[W \text{ SHR } 4] \text{ AND } 0FFFh] - 2048) \cdot 20.0 / G) / 4096,$$

where SHR denotes logical right shift and G is the gain used. This formula is valid for use in bipolar input mode only.

The data transfer from the board to the PC can take place in one of four different modes, which are supported by the driver software.

- In *'single mode'*, the board acquires a single sample from an analog input channel, with a given gain setting, and returns it to the calling progam.
- In *'synchronous mode'*, the board acquires a single sample or multiple samples from one or more analog input channels. The calling program is halted, until the specified number of samples have been acquired.
- In *'interrupt mode'*, the board acquires a single sample or multiple samples from one or more analog input channels. The device driver initiates the conversion and then returns control to the calling program. The board generates an interrupt after each A/D conversion. The called interrupt routine should transfer the sample from the board into memory.
- In *'DMA mode'* , the board acquires a single sample or multiple samples from one or more analog input channels. The device driver initiates the conversion and then returns control to the calling program. The board writes data directly to memory, using the PC's DMA controller. DMA mode is faster than interrupt mode, because the actual data transfer is not controlled by the CPU. Processes on the CPU can continue.

2.4 Interfacing to the Relaxograph

The interfacing of the Relaxograph to a PC has been described extensively by Smans. The Relaxograph has two outputs: one analog output for the EMG and triggering signals, and one RS-232 serial data output. The digital output exports the twitch heights calculated by the Relaxograph and some status information to the PC. The status information concerns several internal alarms ('electrode off' and 'HF disturbance') With respect to Smans, a few changes were made to the link.

2.4.1 Relaxograph trigger signal

Before, the signal that is called 'NMT response' (pin 4) was used as a trigger signal. It was discovered that this signal does change on the moment of stimulation, but its amplitude is proportional to the EMG response. This means that it is almost zero when the patient's muscles are relaxed completely. Although Smans did not report any problems, in our setup this led to loss of triggering. It is suspected that the implementation of the 'NMT response' signal in the version of the Relaxograph which Smans used differs from our version.

In any case, from the Relaxograph electrical circuit schemes [Datex NMT-100 technical manual monitor, 1985], it was clear that a certain signal line in the stimulation circuitry would provide better trigger information[1]. The signal is used internally to open a noise gate placed before the input of the EMG amplifier. This gate is opened 0.5 seconds before the first as well as 0.5 seconds after the last stimulus of a TOF, to measure the noise or HF-interference level. It is also open from 3 to 18 ms after each stimulus. The normal level (gate closed) is 0.7V, and the active level (gate open) is -12.2 V. After switching the Relaxograph on, the level is -12.2 V. When after that, the stimulator is turned on, the level changes to 0.7V.

2.4.2 Analog EMG output

The Relaxograph amplifies the EMG signal and filters it with a bandpass filter, which was specified to have 60 Hz and 400 Hz cut-off frequencies. The EMG signal was sampled by the Labmaster A/D board at a 50 kS/s rate and low-pass filtered with a digital moving average filter with a 540 Hz cut-off frequency that will be described in paragraph 2.5. The resulting over-all frequency transfer function is a band pass filter with 60 and 400 Hz cut-off frequencies.

2.4.3 Serial data link

For the serial data link wiring and protocol, the interested reader may refer to [Smans 1993]. The following extra features that were not described in the manual were noted:
When turned on, the Relaxograph sends a character FFh, and when switched off, the Relaxograph sends a character 00h. This feature has been utilized in the software (see next chapter).

2.5 Interfacing to AS/3 ADU

There are several ways to receive measured data from the AS/3 ADU. There is a high-speed serial link (119.200 baud), that uses an advanced protocol for the interfacing to many physiological parameters. It also provides on-line access to several types of digitized raw waveforms, like the ECG and capnogram. Unfortunately, the NMT's EMG waveforms are not among these types.

Another possibility to receive raw data (including the NMT measurements) is via the so-called UPI board connector. The ADU can be configured to export several waveforms via this connector[2]. In this way, up to 16 different signals are available in analog form, with voltages between -5 and +5V. In a first test, it was noted that the signals are not the actual analog signals, but internally D/A converted versions of A/D converted measurements.

---

[1] The signal used as a NMT trigger runs from the collector of transistor V26 to the gates of FETs V2 and V25, and is marked **D** on the printed circuit board. It was connected to pen 8 of the analog output via a 1 KΩ resistor. The modification was approved by the Catharina Hospital medical instrumentation service.
[2]For this purpose, two passwords need to be entered in the 'monitor setup' menu.

2.5.1 AS/3 ADU data acquisition chain for NMT signals

It was found that the signals are 'stepped' due to quantization errors and because the monitor's D/A converter is not followed by a low-pass filter. More important, the D/A conversion takes place at another rate than the A/D conversion. This means that the signals at the output are 'scaled' in time.

These signal properties may however be overcome if the PC samples the signal at an adjusted rate, and uses a digital low-pass filter to round of the 'stepped' signal.

The internal signal processing chain from EMG electrode to the UPI board output, together with the adapted PC acquisition system are shown in figure 2.3.

In the AS/3 ADU the EMG signal from 3 to 18 ms after the stimulus is amplified, band pass filterered from 60 to 400 Hz, and converted at a 2.5 kS/s rate for internal storage. This signal is then converted back to an analog signal at a 100 S/s rate (25 times slower), that is sampled by the Keithley A/D board at a 3000 S/s rate. It was noted that after each 375 ms response, the sample & hold circuit of the monitor's D/A convertor kept the output fixed at the last encountered voltage.

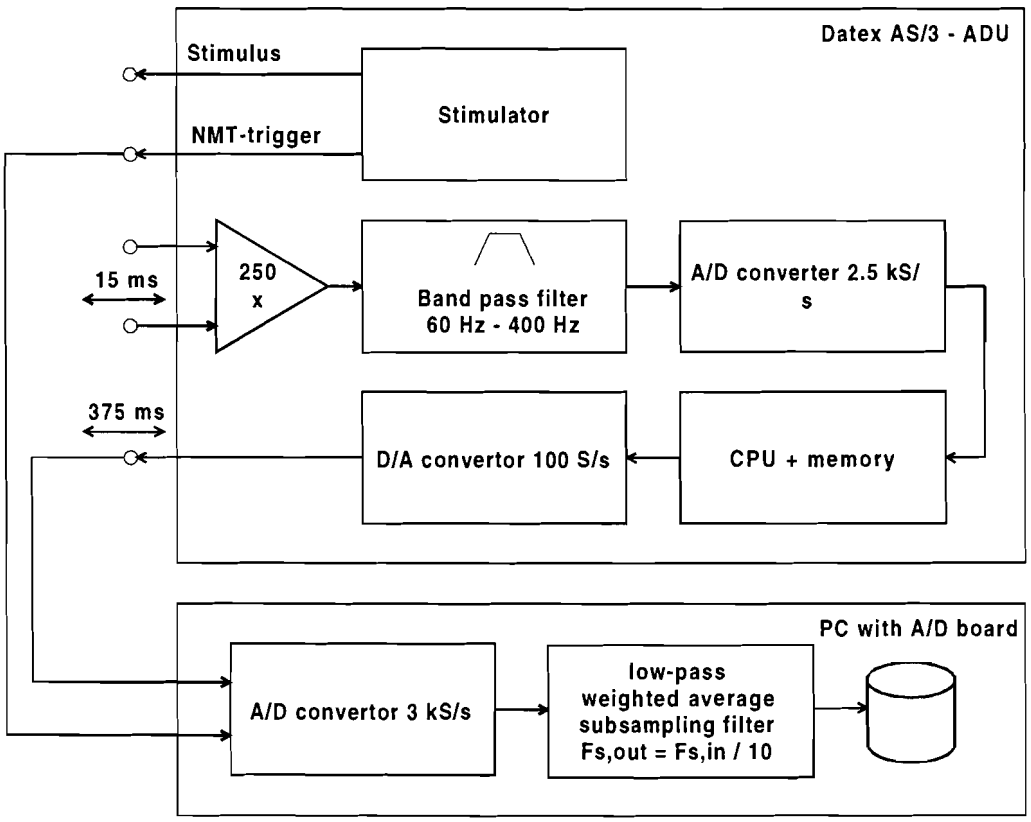

Figure 2.4 - Signal processing chain using AS/3 monitor and PC

In this way, the sample frequency of the EMG signal at the input of the A/D conversion board becomes 3000 x 25 = 75 kHz. This 30 times oversampling was used to avoid distortion of the signal due to timing errors related to the step-wise changes in the AS/3 output signal. The A/D board could not be synchronized with the ADU's D/A convertor.

Finally the signal is low-pass filtered and subsampled by the acquisition program on the PC. The transfer function of the moving average filter is depicted in figure 2.4. This filter is the same as the one used by Smans [Smans 1993]. It has a cut-off frequency (-3dB) of 0.0108·sample frequency, which results in 810.5 Hz. Since the bandwidth of the signal is now only about 2% of the Nyquist frequency, samples may be left out without loss of information. This is done by the subsampling filter, that outputs 1 out of each 10 successive input samples. The filtered version is stored on disk. The sample frequency of the stored signals is 7500 Hz.

The implementation of both filters was combined by calculating the response of the moving average filter only for the samples that are output by the subsampling filter.

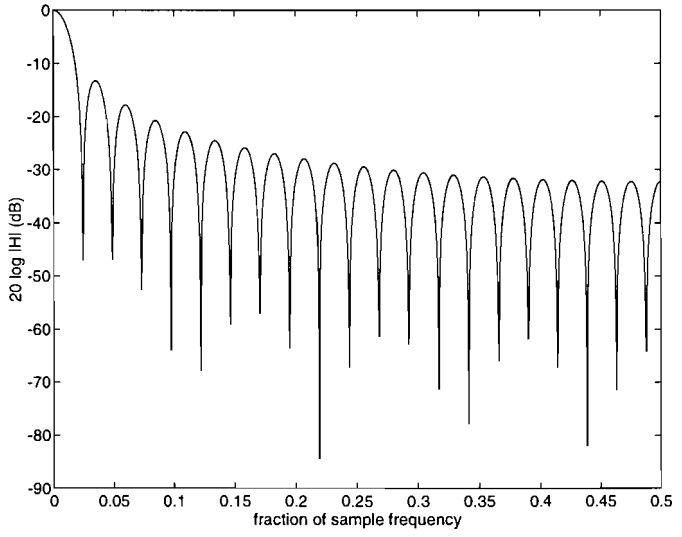

Figure 2.5 - Transfer function of the 41 point moving average filter. In the Relaxograph version, the sample frequency before filtering is 50 kHz, while in the AS/3 version, the sample frequency before filtering is 75 kHz.

2.5.2 AS/3 ADU NMT trigger signal

A second output on the UPI board was configured to output an NMT trigger signal. This signal is normally 0V, and changes to +5V at the start of each TOF. It stays high during 1.510 seconds. The trigger goes low before the last response has faded.

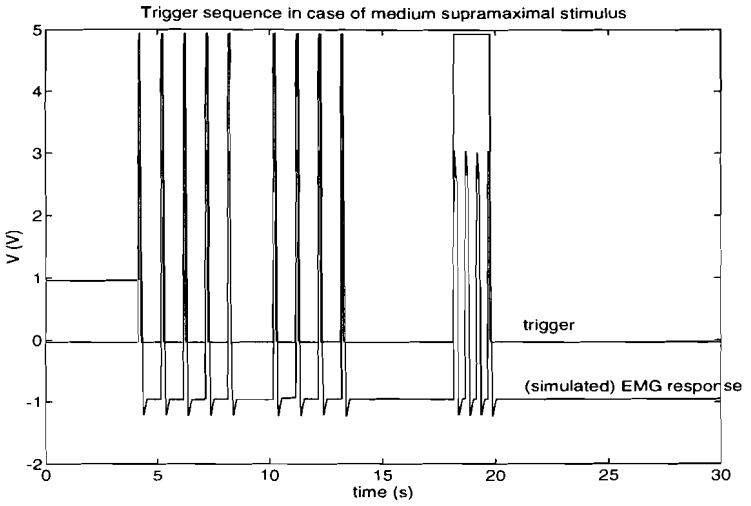

Figure 2.6 - Calibration cycle of NMT in AS/3 ADU with NMT simulator connected. The simulator's response duration is 11 ms in real time. In this case it takes five stimuli to find the supramaximal stimulation level. The second group of four twitches is the reference measurement. During calibration, the trigger goes high for every stimulation. In normal operation, there is one trigger for every train-of-four.

The calibration cycle of the AS/3 ADU differs slightly from the Relaxograph's calibration cycle. It is shown in figure 2.5. In this figure, the response of an NMT simulator connected to the NMT input is shown together with the NMT trigger signal.

3. Software of the measurement system

3.1 Design method

The software has been designed in a modular fashion using structured programming techniques in Borland Pascal, based on program modules called 'units'. This lead to a number of units corresponding to the various tasks and physical parts of the system. A very important design task was to choose a logical and consistent structure of units. After that, the units were designed and tested separately.

In order to produce a readable and maintainable program, the following programming rules have been obeyed:

1. All variables in units are invisible outside of the unit. To get data out of or into a unit, the user calls procedures or functions that return the data via their parameters.
2. Inside the units, variables may be shared. This helps to keep the number of parameters low, because the procedures and functions may access this data directly.
3. Datatypes are defined in the units that produce data of these types.
4. Some naming conventions are obeyed in the whole program:
    - All types, procedures and functions that a unit shares with the outside world have a two letter prefix, indicating the unit, followed by an underscore. For example, the `SC_MsgBox` function is in the screen unit. It displays a message in a rectangle and asks the user for input. It returns an `SC_MsgBoxType` variable to indicate the user's choice.
    - Constants have a prefix indicating either the unit or the procedure they are used in. For example: `SC_MsgBox` returns `MSG_OK` if the user selected 'OK' in response to the messagebox.

3.2 Survey of the units

Figure 3.1 shows the hierarchical organisation of the units of the control system. Test programs have been written to show the capabilities and the way to invoke their functions. Two versions of the program have been developed. The Relaxograph version interfaces to the Relaxograph NMT-100, while the AS/3 version interfaces to the AS/3 ADU. The names of the AS/3 version units are preceded by *AS3_*. A short description of the functionality of each unit now follows.

The raw EMG, available on the NMT's analog output is first sampled by the *AD_Routines* unit. This unit returns raw twitch data of type `AD_TwitchType`. It takes care of the communication with the A/D board via a driver library. The triggering of the measurements is done by software in this unit.

The main purpose of the *EMG_Processing* unit is to process the raw signal. The signal is filtered and sub sampled using a 41 point moving average and subsampling filter, as described in paragraph 2.5.1. Several simple parameters of each twitch (rectified integrated EMG, maximum, minimum) and of each TOF (T_4/T_1, T_1/T_{ref}) are calculated. The train-of-four data can be exported as `EP_TOFType` records and as a formatted string that can be put on screen directly.

The serial data calculated by the Relaxograph are received over a serial communications link. A low-level communications driver, contained in the *RS232* unit, serves to receive and send bytes

out to two RS232-ports. The RS232 unit contains character level serial interface routines to communicate with the Relaxograph and the pump via COM1 and COM2. Since MS-DOS does not support serial communications with no handshaking using a three wire cable, standard DOS interrupt service routines could not be used. A new interrupt service routine is installed that stores the incoming characters in a rotating local buffer. A flag is set to indicate if data is available to the rest of the program. This unit has no function in the AS/3 version.

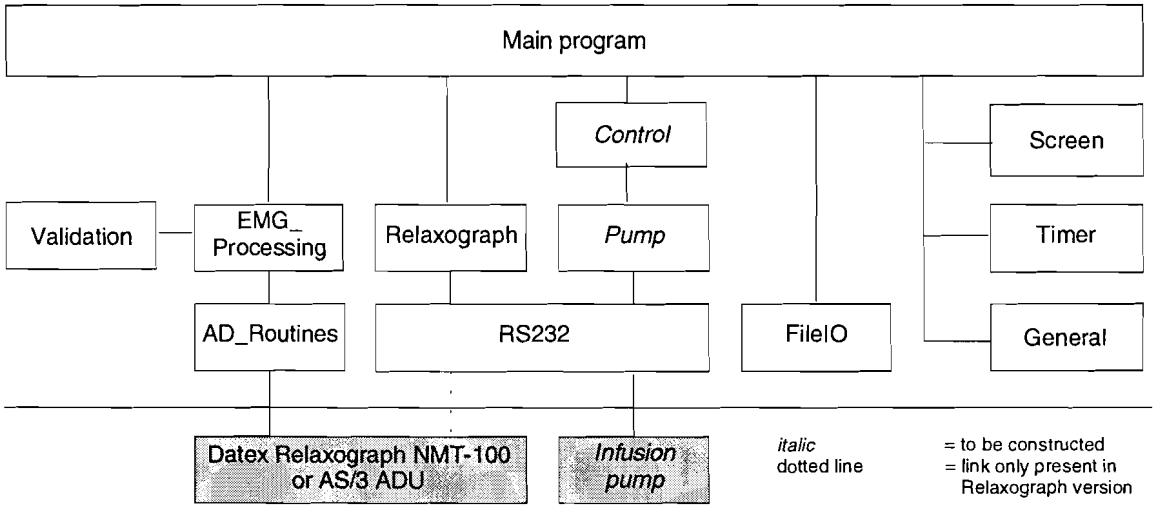

Figure 3.1 - Unit hierarchy proposed for the final controller program. Blocks with a gray background are hardware.

The *Relaxograph* unit serves as a shell around the RS232 unit that handles the Relaxograph's serial communications protocol and keeps track of its current state. It can return the serial data in a data structure of type `RE_RelaxogrType` as well as in a formatted string, that is suitable for screen output. It also keeps track of the operating mode of the Relaxograph (as well as possible). In the AS/3 version, this unit is only used to convert a recorded `RE_RelaxogrType` record into a formatted string.

The *Pump* unit will implement the infusion pump protocol. It also uses the RS232 unit to send and receive information from the computer controlled infusion pump via a second serial link. This unit is still to be constructed. Probably a unit previously developed for the blood pressure control system can be used.

The *Control* unit will calculate the amount of pharmacon to be infused, based on the last measurement data. It may also adapt the parameters of a pharmacodynamic / pharmacokinetic patient model. The output of that model can be used when a measurement is invalid. Several decision rules should be implemented, so that the Control unit can monitor its performance and take action if necesary. This unit will also be a topic for further investigation.

The *FileIO* unit serves to read and write the analog and serial measurements from and to the hard disk. When a previously recorded file should be read, first a list of files is displayed of which the user may choose one. Before starting measurements, the unit asks for a filename. If no filename is entered, the measurements will not be stored on disk.

The *Screen* unit provides a set of routines to display EMG measurements graphically and to show messages to the user. It can display a 'message box', an 'input box', 'text boxes', a 'menu box', a large screen title and many sorts of graphs (line, point, bar, with or without axes) in a flexible and user-friendly way. The graphs can be defined using an `SC_GraphType` record.

The *Timer* unit contains time handling functions. It can return the current time and uses the PC's timer interrupt for a time-out routine. This routine is used to monitor the progress of measurements.

Finally, the *General* unit contains several general purpose functions, especially string formatting functions, that can be used by all other units.

4. Validation methods for TOF signals

In this chapter a method to develop a statistical validation algorithm for TOF signals will be proposed. First we will define the demands to a validation algorithm. Then several possible methods for validation will be described, and one will be chosen. The chapter is concluded with a more detailed description of that method.

4.1 Demands to a validation algorithm

There are several criteria to be met for the algorithm to be useful in clinical practice [de Graaf 1993]. First, the algorithm should recognize all measurements that an expert (for example, an anaesthesist) would consider invalid. Second, the number of measurements that is considered invalid by the algorithm while being considered valid by an expert should not be too high.
The main property of a good validation method is, that the number of invalid measurements that is considered valid by the algorithm is minimal. This is important because every such measurement may trigger a false alarm or cause a wrong control action. Most of the time, the number of valid measurements considered invalid by the algorithm does not have to be very low. The need for information of the control algorithm, in terms of valid measurements per unit of time, will be discussed below.
A prerequisite constraint to the algorithm is that the algorithm should be fast enough to validate the signals in real time on a PC. Since there are 18 seconds between each two successive measurements, the maximum time available for the validation is in the order of a few seconds per measurement.

4.1.1 Maximum number of subsequent invalid measurements

It depends on the control algorithm, and on the phase of the relaxation (onset, steady state or recovery) how many measurements may be unusable before the control performance gets in danger.
The limit to the maximum number of measurements that may successively be missing follows from the Nyquist criterium. The sample frequency (i.e. the number of *valid* TOF measurements per unit of time) should be twice the highest frequency in the signal. Since the response to the muscle relaxant drug is a strongly non-linear process, this frequency is different during the different phases of action.

During the onset of relaxation (see figure 4.1), the level of muscle relaxation changes very rapidly. After injection, the patient's response normally stays at 100% for 1.5 to 3 minutes. After that, within 1 minute (i.e. 3 TOF measurements) the response goes from 100% to a value of about 0%. In this phase, the maximum sample frequency of 3 measurements per minute is actually not high enough. So in this phase, in theory the controller has only very little control over the patient, because it does not have enough data.

After the onset phase, a steady state phase starts. In this phase the level of relaxation stays more or less constant. Of course, when the muscle relaxant control system is used, the level of relaxation will be kept as constant as possible. In this phase, the dominant time constant is related to the duration of action of the muscle relaxant drug used. This time constant is in the order of 27 (standard deviation = 5.0) minutes for vecuronium to circa 10 minutes for mivacurium. This means that 1 valid measurement every 5 minutes would be enough. However, in order to have a

margin to improve the controller's performance, a limit of one valid measurement per minute is proposed in the steady state phase.

Recovery of muscle relaxation is a slower process than the onset. Here the same limit applies as in steady state. Because of these considerations, the maximal number of subsequently invalid measurements is 0 in the onset phase, and 5 in the steady state phase.

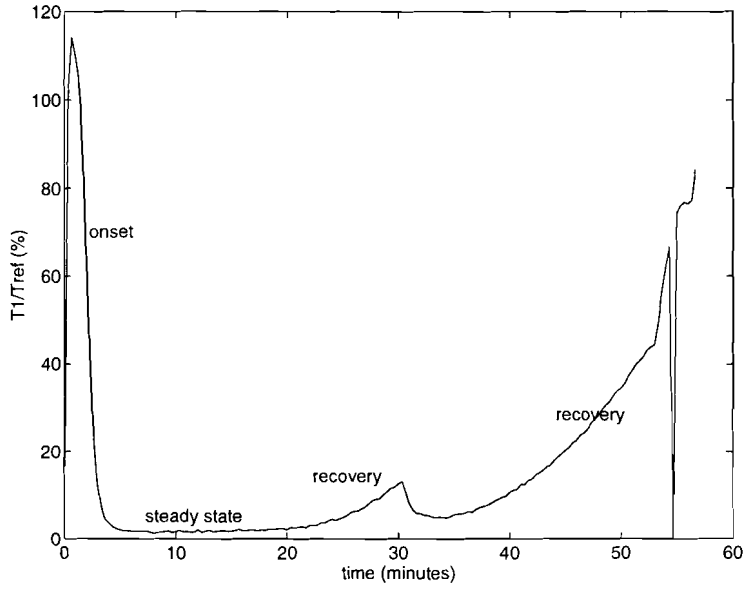

Figure 4.1 - Phases in the course of action of vecuronium. After 30 minutes, a new smaller bolus dose was given. After 55 minutes the measurement was disturbed.

4.2 Possible methods for validation

From literature, several possible strategies arise to meet the given demands.

4.2.1 Petri nets

A Petri net was used to validate arterial blood pressure signals. Extrema (significant points) of the signal are determined, and the slopes of the periods in between. It is assumed that in valid signals, these points and slopes always occur in a known order. This order can be represented by a state diagram (called Petri net). Any transition of a measured signal that is not within this diagram, is to be considered invalid. Although this method works well for signals with a well-defined shape, it is not very useful for validation of muscle relaxation measurements [Smans 1993], because the exact EMG waveform depends on too many factors, and changes dramatically in function of the level of muscle relaxation.

4.2.2 'Map' method

Two different approaches are presented by de Graaf [de Graaf 1993]. The first is called the 'map method'. It checks whether a piece-wise linear approximation of a measured waveform lies within the borders, drawn around a piece-wise linear approximation of an 'ideal' valid reference measurement.

First, significant points are abstracted from the reference signal. A simplified version is then generated by linear interpolation between these points. Upper- and under limit borders are calculated that run in parallel to the curve at a given perpendicular distance.
Of every measured signal, the simplified representation is calculated, and it is checked to the borders. If the representation lies completely within the borders, it is considered valid, else it is called invalid.
In case of muscle relaxation measurements, the 'ideal reference measurement' should probably be chosen as the last measurement. A problem with the application of this method to muscle relaxation signals is, that rapid signal changes may be valid.

4.2.3 Linguistic method

The second method that de Graaf proposes is a 'linguistic' method. The measured signal is again simplified into a piece-wise linear approximation. Each line segment is then characterized by its slope and length. Each combination of slope and length is given a letter code, so each line segment is assigned a letter. Placed one after another these letters form 'words' for each wave. A list ('dictionary') can be made of all valid words. If the word belonging to a given signal is not in the dictionary, that signal is considered invalid. However, it turned out that rather similar signals could yield different words.
In our case, this would probably yield large problems with the small, noise-like signals in case of deep levels of muscle relaxation. Moreover, the words belonging to these signals are likely to be very different in length.

4.2.4 Artificial neural networks

Yet another method would be the use of artificial neural networks. Since the validation can be seen as a classification problem, neural networks might be helpful. However, this approach has the serious drawback, that the decision of the network cannot be reduced to physiological knowledge; the network cannot tell why a certain measurement was considered valid or invalid.

4.2.5 Heuristic method

The method that will be used in this work, could be called a heuristic approach to validation. It results from the observations that the shape of the TOF signals depends on the level of muscle relaxation, that the signal shape varies between patients, and that the signals are noise-like in case of deep levels of relaxation.
First, recorded TOF measurements are analyzed by eye in order to gain knowledge about the signals and artefacts. Then, from the learning set many parameters and their probability distributions are derived. It is expected that the parameter value distributions are gaussian, with 'outliers' caused by artefacts. Based on these distributions, suitable criteria may be derived. A measurement is considered valid only if all parameters satisfy the criteria. The algorithm can be optimized by letting it judge the learning set of measurements. If the results are satisfactory, the final algorithm can be tested on a set of independent test data.

The algorithm will base its decision on clear criteria, and will be able to tell why a measurement was considered invalid. Depending on the reason for invalidation, the measurement might simply be rejected, the clinician might be advised to correct the cause of the artefact (e.g. in case of direct stimulation of muscles), or, in some cases the artefact could perhaps be corrected for.

The parameter set may include continuous signal properties like amplitude and duration, as well as discrete properties like the number of zero crossings. Boolean parameters that are the result of more complex algorithms may also be used.

The following groups of parameters are proposed:

I. parameters based on the shape of a single twitch, for example the amplitudes and latencies of peaks in the signal,

II. parameters based on the speed of variation of the shape: since the muscle relaxation, and probably also other parameters do not vary rapidly (especially in the steady state phase), the rate of change of these parameters should lie within narrow bounds. The rate of change can be considered for parameters:
   A. within one TOF (for example ratios of peak-to-peak values),
   B. between subsequent TOFs.

In this way, we hope to find and make use of constancies and / or reproducible features in the signal. These constancies and reproducibilities constitute the 'knowledge' about correct TOF signals.

Thus, the Heuristic approach to validation, used in this work, may be summarized as follows:

1. Inspect a learning set and a test set of measurements by eye. In this way, a 'golden standard' is determined for the validation algorithm, and insight in signal properties and artefacts may be gained.
2. Choose (a large number of) parameters that are based on a single twitch, on the rate of change between the twitches of one TOF, or on the rate of change between TOFs.
3. Calculate the parameters for every measurement in the learning set. The results are presented in histograms.
4. Determine suitable criteria for the parameters.
5. Apply the criteria to the learning set and compare the results to the results of the visual inspection.
6. Verify the algorithm with a test set of measurements that is independent of the learning set.
7. If necessary, the algorithm should be optimized by repeating steps 2 through 6 until the results are satisfactory. To assure the independency of the test set, a new test set should be acquired and used in the iteration.

The analysis and selection of parameters and the determination of criteria (steps 1, 2, 3 and 4) are the topic of the next chapter. Chapter 6 presents the results of applying these criteria to the learning set and to the test set (steps 5 and 6).

5. Parameter analyses

In this chapter, an extended analysis of the data in the learning set is presented. A brief description of the learning set will be given in paragraph 1. Some parameters for a single ECAP response will be shown in paragraphs 2 and 3. In the fourth paragraph, the relationships between the parameters of different ECAPs (within a train-of-four and between one ECAP and the reference ECAP) are explored. In the fifth paragraph the time course of some parameters is discussed. The final paragraph shows the relationship of some signal parameters and the T_1/T_{ref} ratio.

5.1 The learning set

The learning set consisted of circa 6878 train-of-four measurements containing 27512 EMG responses that were collected during 30 surgical operations in the Eindhoven Catharina Hospital for a previous work of Joost Smans. Since the main goal of that work was to determine correct electrode placements, the positions of the stimulating as well as of the measuring electrodes were different in each operation, and sometimes the electrodes were moved during an operation. For that reason, the measurement files may contain more unusable TOFs than in normal clinical practice. Moreover, due to the different electrode positions, the shape of the EMGs varies strongly. It is expected that this variation will be smaller when the positions are chosen optimally, but by training with this varied test set, the algorithm will be prepared for non-optimal electrode positions, too.

A LabMaster data-acquisition board was used for data acquisition. Preprocessing consisted of a subsampling and interpolating filter that left 100 samples per twitch, as described earlier.
The voltages presented here are the voltages on the Relaxograph's output. On this output, the EMG-signal was amplified 1000 times, and bandpass filtered to eliminate 50 Hz noise. Every volt in the histograms corresponds to 1 mV in the EMG signal.

The operations were done under several different anaesthetic conditions. The muscle relaxant used most of the times was vecuronium.
During manual examination of the measurement files the following minor technical imperfections were found:

- the four control twitches were triggered 1.0 ms late, compared to the subsequent twitches;
- in a few cases, the gain had not been adjusted correctly so the tops of the ECAPs were chopped off;
- sometimes triggering was incorrect, so that in these cases the first twitch was recorded as the second.

The distorted measurements were included in order to test the ability of the validation algorithm to discern technical errors.

The only indication of noise or HF-disturbance, recorded in the measurement files are a noise number and the HF-disturbance and electrode-off flags given by the Relaxograph. But since it was not clear how this information was derived, and since the electrodes-off information was only updated after every 6th TOF (so only once in every 2 minutes), it is hard to use for validation purposes.

5.2 Amplitude related parameters of single ECAPs

First, second, third and fourth ECAPs of every train-of-four have been analyzed separately. Mean value and standard deviation have been calculated over all four ECAPs.
In order to show more detail, only the relevant parts of the histograms are depictured. In each case, more than 95% of the parameter values are represented in every histogram.

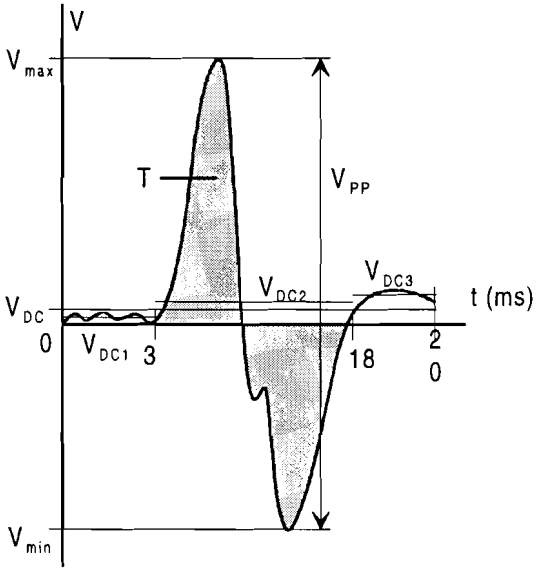

Figure 5.1 - Amplitude related parameters: T, V_{DC}, V_{DC1}, V_{DC2}, V_{DC3}, V_{max}, V_{min} and V_{PP}.

5.2.1 T - Integrated rectified value

The T parameter was computed using the following formula:

$$T = \frac{0.015}{N_s} \sum_{n=0.003 \cdot N_s/0.020}^{0.018 \cdot N_s/0.020} |v_n| \ .$$

So each ECAP was rectified and summated from 3 to 18 ms (grey area in figure 5.1). The sum is made independent on the duration (15 ms) and the number of samples. This time period was taken because before 3 ms, a stimulus artefact may be present, and after 18 ms the signal is more or less random.

The theoretical maximum value of T is 200 mVs (=10V · 20 ms). No T values above 80.5 mVs were found. The high maximum T values for ECAP 3 were due to artefacts. Since these TOFs did have a well behaved ECAP 1 they were not scored valid during the visual inspection.
The larger T values belonging to the 'unrelaxed' state in the beginnings of the operations are not visible, since their values range from 10 to 81 mVs. Since the distribution of this parameter is not a gaussian one, no standard deviation has been calculated.
We must conclude that this parameter depends on the relaxation level, and is only useful for validation with very wide bounds. The value T = 0 Vs is not expected because there is always some background noise present.

Table 5.1 - Mean and maximum of T values (all values in $\cdot 10^3$ Vs)

	ECAP 1	ECAP 2	ECAP 3	ECAP 4
Average value	4.3401	2.2846	1.8428	1.7554
Max	32.070	42.305	80.546	31.938
Max of TOFs scored 'valid'	32.070	31.846	78.816	31.938

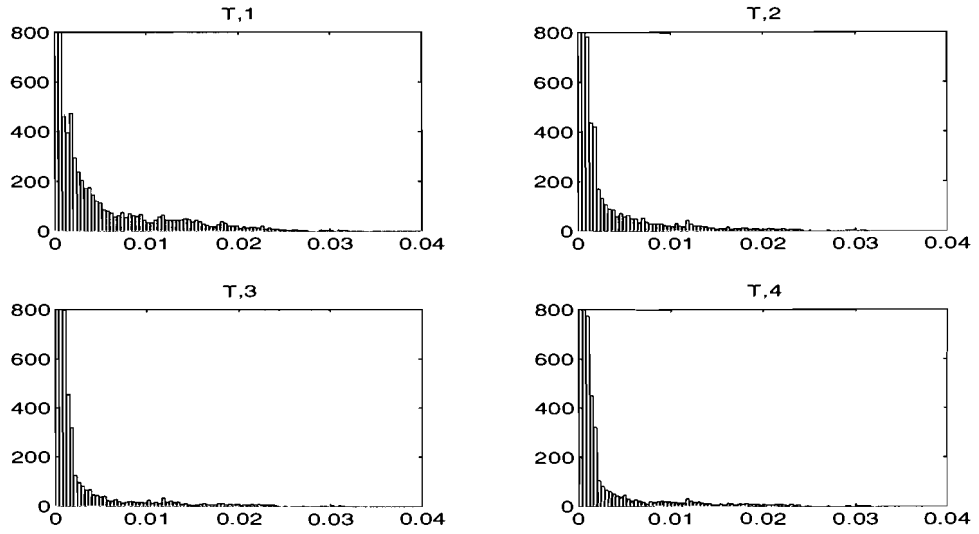

Figure 5.2-Histograms of integrated rectified values (in Vs) of all four ECAPs. Average value 2.6 mVs, standard deviation 4.4 mVs. Count per bin limited to 800.

5.2.2 V_{DC} - Average voltages

The reason for looking at DC components was that they might be good indicators of direct stimulation. It is supposed that direct stimulation causes unipolar exponential waveforms with a negative DC component. Moreover, technical failures may lead to higher DC levels.
The DC component was determined over the complete ECAP and over three different parts of the ECAP (see figure 5.1). The three parts correspond to the 'stimulus artefact', 'biphasic action potential' and 'afterwave' time windows.

The average DC voltage over a whole ECAP (from 0 to 20 ms) is circa zero, as can be seen in the histograms. The histograms do show a peak at 20 mV, but apart from that, V_{DC} seems to be distributed normally, with some 'unproper' values at the extremes (at -0.08 V and at +0.08 V). Examination of the concerning TOFs showed a constant DC offset voltage that was probably due to the amplifier or Labmaster A/D board. Only a fraction of these TOFs was disturbed by direct stimulation.

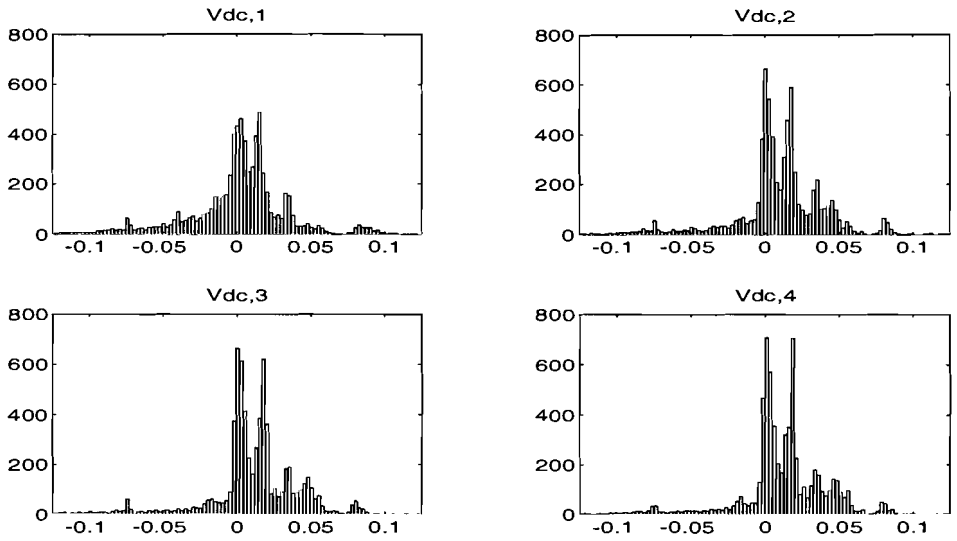

Figure 5.3 - Histograms of average DC voltage (in V) of ECAPs 1 to 4. Average value 7.2 mV, standard deviation 38.0 mV.

Table 5.2 - More statistical data on V_{DC} (values in V)

	ECAP 1	ECAP 2	ECAP 3	ECAP 4
Average value	-0.000211	0.00847	0.0104	0.0103
Minimum	-0.2433	-0.3659	-0.3357	-0.3401
Min. of TOFs scored 'valid'	-0.2300	-0.2279	-0.3357	-0.3401
Maximum	0.7672	2.087	0.6892	0.2472
Max. of TOFs scored 'valid'	0.7672	0.2864	0.3884	0.1410

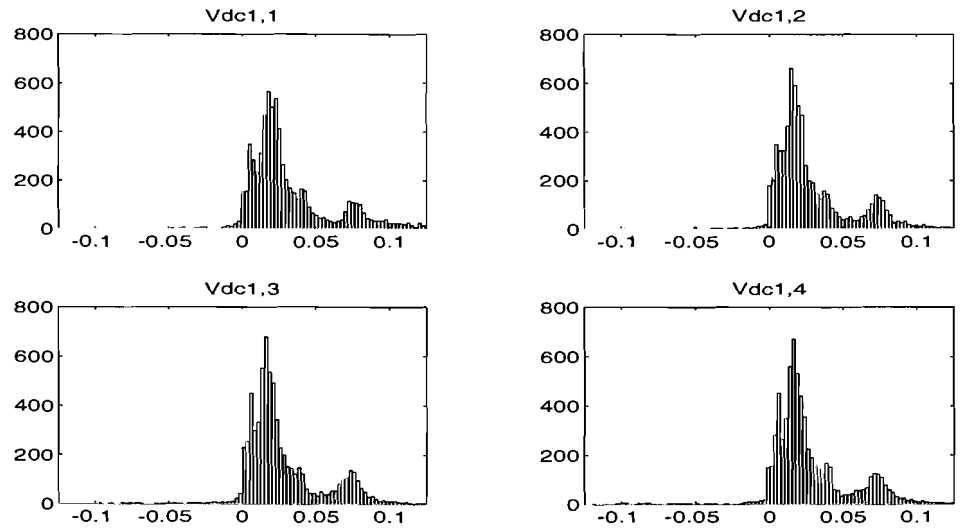

Figure 5.4 - Histograms of average voltage (in V) of ECAPs 1 to 4 in the 0 - 4 ms interval. Average value 30.5 mV, standard deviation 52.6 mV.

The part of the signal between 0 and 4 ms does have a positive DC component, as can be seen in figure 5.4. Peaks occur at circa +15 mV and at +80 mV.

Table 5.3 - More statistical data on V_{DC1} (values in V)

	ECAP 1	ECAP 2	ECAP 3	ECAP 4
Mean	0.0335	0.0297	0.0299	0.0289
Minimum	-0.4634	-0.4612	-0.5201	-0.8124
Minimum of TOFs scored 'valid'	-0.3601	-0.4612	-0.1193	-0.8124
Maximum	0.8818	2.6376	4.5743	0.7087
Maximum of TOFs scored 'valid'	0.8818	0.5425	3.1630	0.7087

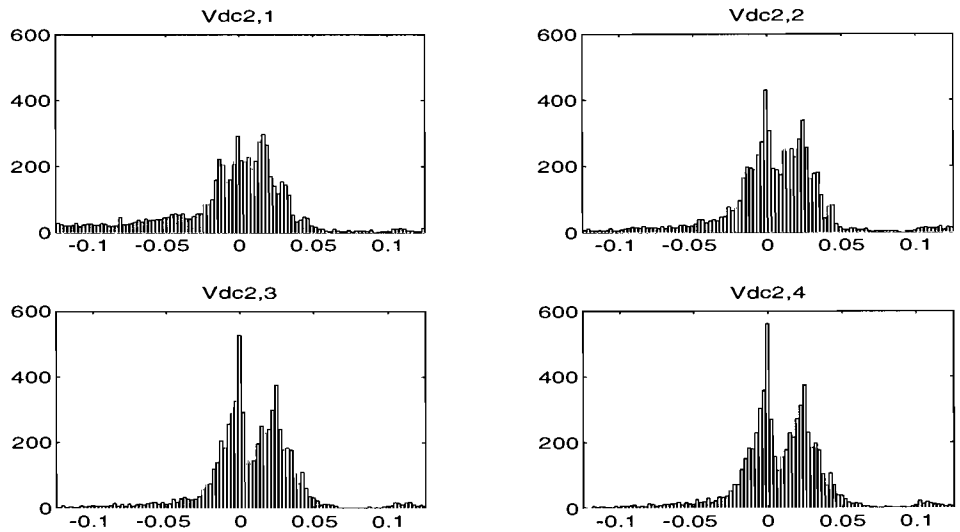

Figure 5.5 - Histograms of the average voltage of ECAPs 1 to 4 in the 4-15 ms interval. Over all mean = -5.0 mV, standard deviation = 66.5 mV.

Table 5.4 - More statistical data on V_{DC2} (values in V)

	ECAP 1	ECAP 2	ECAP 3	ECAP 4
Mean	-0.0172	-0.0031	0.0001	0.0000
Minimum	-0.6198	-0.5573	-0.5892	-0.5967
Minimum of TOFs scored 'valid'	-0.5481	-0.5573	-0.5892	-0.5967
Maximum	1.5349	2.7687	1.6666	0.3562
Maximum of TOFs scored 'valid'	1.5349	0.5938	0.2371	0.3562

In the period from 4 to 15 ms after stimulation (for normal signals this is a biphasic signal) the DC value is expected to be circa 0 V. The histograms of figure 5.5 show that this is true. The histograms are broader (larger deviation) than those from figures 5.4. This is because in the 4-15ms interval, the signal itself deviates stronger from V_{DC2} than it does over the complete 0-20ms interval.

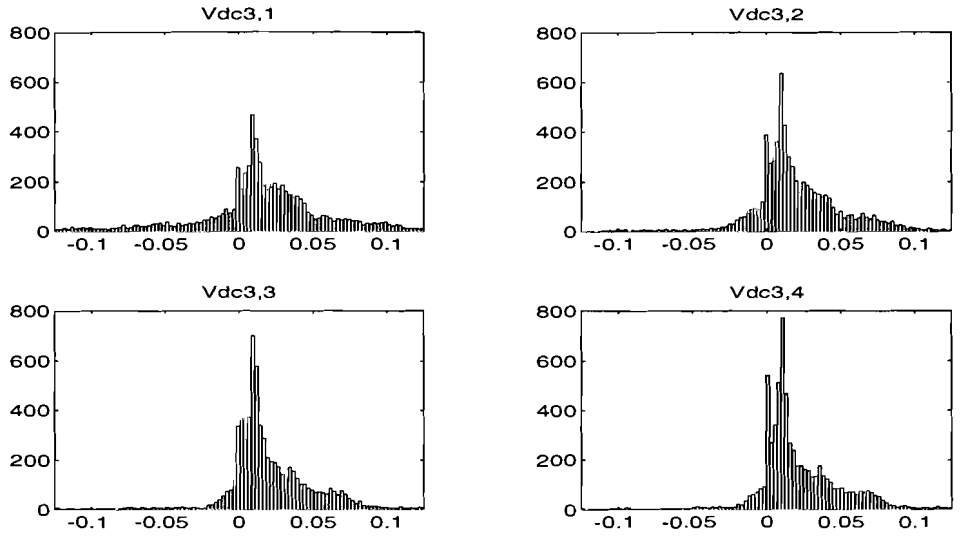

Figure 5.6 - Histograms of the average voltage in the 15-20 ms interval. Over all mean = 17mV, standard deviation = 78.1 mV.

V_{DC3} was determined only in the learning set. The signals in the test set do not contain information after 15 ms from stimulus.

Table 5.5 - More statistical data on V_{DC3} (values in V)

	ECAP 1	ECAP 2	ECAP 3	ECAP 4
Mean	0.0130	0.0181	0.0181	0.0187
Minimum	-1.1895	-1.1664	-4.5269	-1.1181
Minimum of TOFs scored 'valid'	-1.1895	-1.1664	-1.1020	-1.1181
Maximum	0.4782	0.4917	0.6722	0.6877
Maximum of TOFs scored 'valid'	0.3629	0.4427	0.3947	0.6877

5.2.3 Peak to peak voltages

The peak to peak voltages of the several ECAPs were studied because they might be useful for validation in combination with other parameters.

Peak-peak voltages larger than 20 V could not be measured. The peak-peak voltage strongly correlates with the relaxation level. As can be seen in table 5.6, TOFs with a large range of peak-peak voltages have been considered valid during manual validation, so this parameter does not seem to be of use for validation.

Table 5.6 - More statistical data on V_{PP} (values in V)

	ECAP 1	ECAP 2	ECAP 3	ECAP 4
Mean	1.1722	0.6014	0.4725	0.4514
Minimum	0	0	0	0
Minimum of TOFs scored 'valid'	0	0	0	0
Maximum	9.3164	8.7549	10.0098	8.8672
Maximum of TOFs scored 'valid'	9.3164	8.7549	10.0098	8.8672

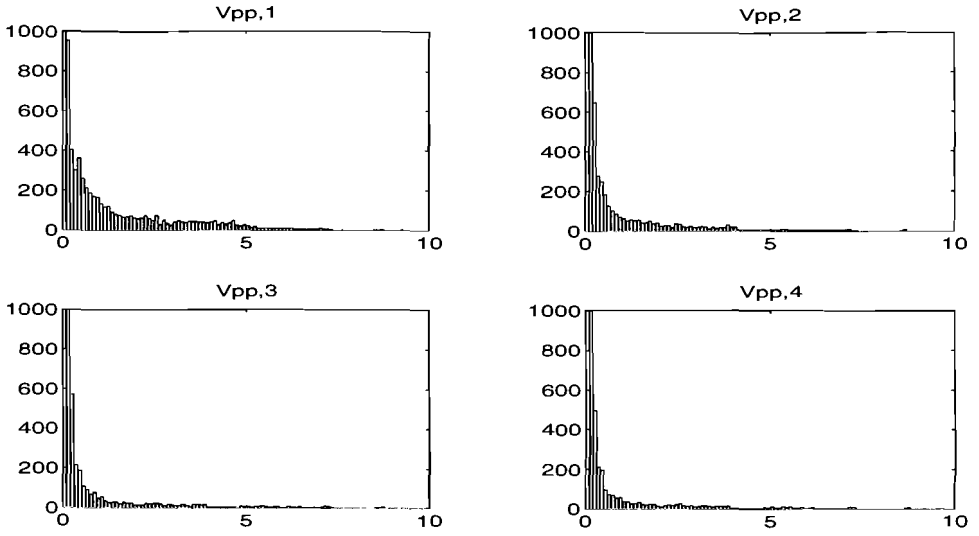

Figure 5.7 - Histograms of the peak to peak voltage (in V) of ECAPs 1 to 4. Average value 0.674 V, standard deviation 1.258 mV.

5.2.4 Ratio of maximum voltage to T

The maximum voltage of an ECAP divided by the area under its curve (V_{MAX}/T) is a measure for how narrow and peak-like the ECAP is. For very steep and narrow ECAPs, this parameter will be large, while broad and flat ECAPs yield small $V_{MAX/T}$ values.
The T value was calculated as discussed earlier. When the T value was very small, the value 0 was assigned the parameter.

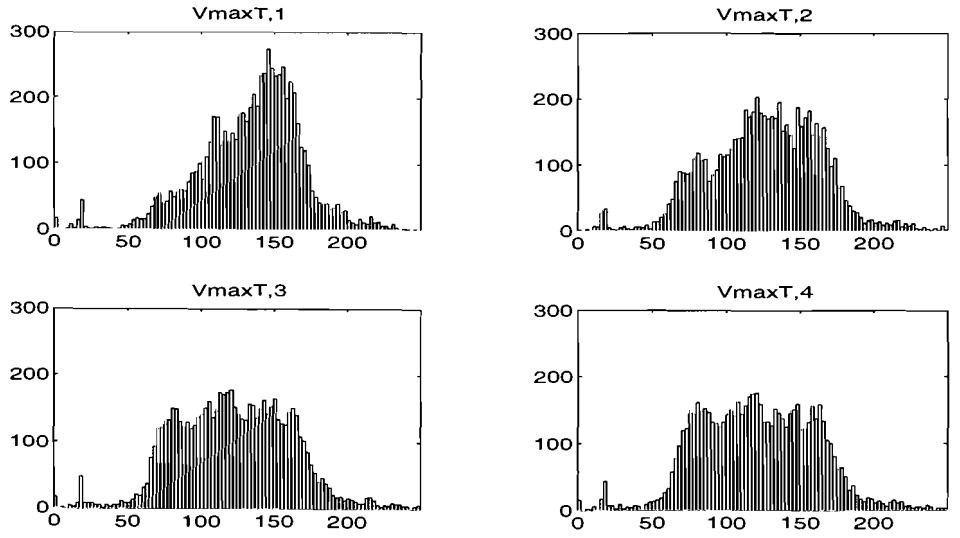

Figure 5.8 - Histograms of the ratio V_{MAX} / T (in s^{-1}) of all four ECAPs. Average value 127 s^{-1}, standard deviation 40.7 s^{-1}.

The histograms show that the parameter usually lies between 50 and 200. The ratio is a little influenced by the level of muscle relaxation. Larger values of the parameter belong to larger T

values (because of sharper peaks), while smaller values belong to smaller T values (broader, more noise-like signals). This parameter can be used for validation, because the maximum value is clearly limited (see table 5.7).

Table 5.7 - More statistical data on V_{MAX}/T (values in s^{-1}, value 0 also assigned when T=0)

	ECAP 1	ECAP 2	ECAP 3	ECAP 4
Mean	134.8167	126.7744	123.0193	122.2937
Minimum	0	-7.3828	-15.4343	0
Minimum of TOFs scored 'valid'	0	0	-15.4343	0
Maximum	1206.9	507.0	366.8	1250.0
Maximum of TOFs scored 'valid'	291.2558	338.9831	304.0425	304.7356

5.2.5 Ratio of minimum voltage to T

The rationale behind this parameter is the same as for $V_{MAX/T}$. It was expected to be more or less equivalent to minus $V_{MAX/T}$. The histograms show that the range of values is comparable to that of $-V_{MAX/T}$, but their shape is a little different.

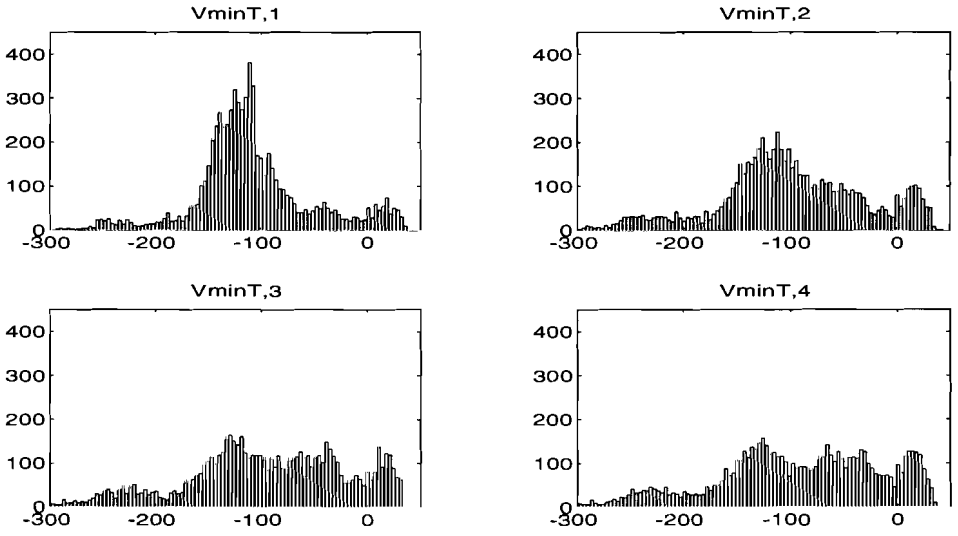

Figure 5.9 - Histograms of the ratio V_{MIN} / T of all four ECAPs. Average value -98.9 s^{-1}, standard deviation 69.7 s^{-1}.

Table 5.8 - More statistical data on V_{MIN}/T (values in s^{-1}, value 0 also assigned when T=0)

	ECAP 1	ECAP 2	ECAP 3	ECAP 4
Mean	-108.4361	-99.9614	-94.0276	-92.9844
Minimum	-371.7472	-358.6498	-362.1908	-358.1662
Minimum of TOFs scored 'valid'	-371.7472	-358.6498	-362.1908	-358.1662
Maximum	39.2066	45.5836	36.3306	38.0360
Maximum of TOFs scored 'valid'	36.6894	36.8939	36.3306	38.0360

5.2.6 Ratio of peak-peak voltage to T

V_{PP}/T is expected to combine the above two parameters. As can be seen in table 5.9, there is a clear maximum to this parameter of circa 530 s^{-1}, that can be used for validation.

Table 5.9 - More statistical data on V_{PP} / T (values in s^{-1}, value 0 also assigned when T=0)

	ECAP 1	ECAP 2	ECAP 3	ECAP 4
Mean	243.3	226.7	217.0	215.3
Minimum	0	0	0	0
Minimum of TOFs scored 'valid'	0	0	0	0
Maximum	1206.9	524.5	506.8	1250
Maximum of TOFs scored 'valid'	528.3	523.7	506.8	533.5

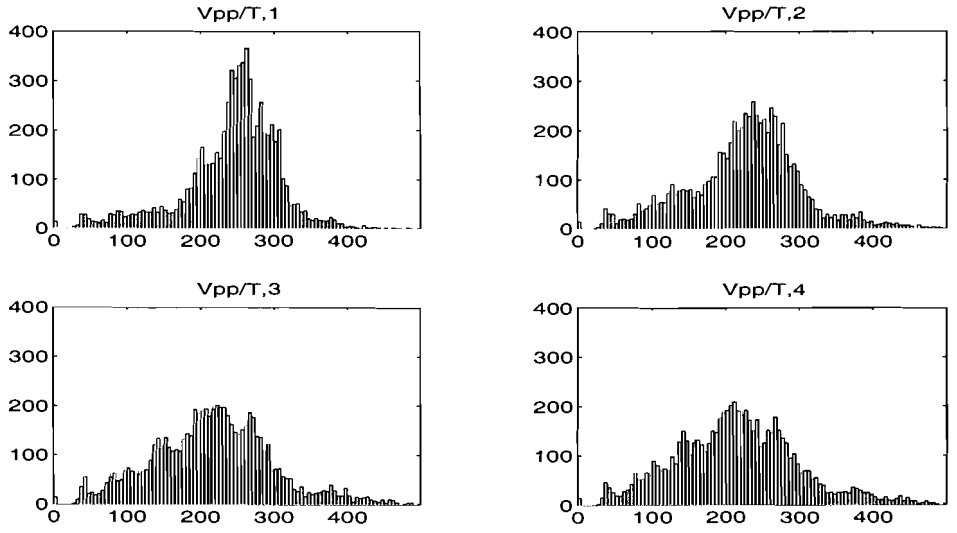

Figure 5.10 - Histograms of the ratio of peak to peak voltage to T of all four ECAPs. Average value 226 s^{-1}, standard deviation 78.9 s^{-1}.

5.2.7 Ratio of DC- to peak-to-peak voltage

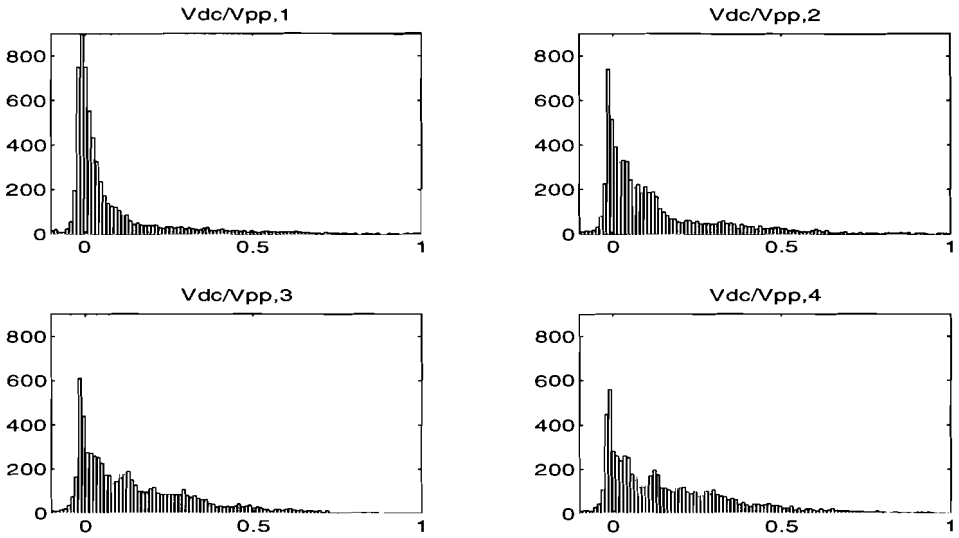

Figure 5.11- Histograms of the ratio V_{DC} / V_{PP} of ECAPs 1 to 4. Average value 0.139, standard deviation 0.2342.

This ratio was expected to correlate with direct stimulation, because in such signals, the DC component was not 0V. However, only the V_{DC}/V_{PP} parameter of ECAP 1 could be used for validation, since for values <-1.5 and >1.5 a majority of the measurements was invalid. No such boundary values could be found for the V_{DC}/V_{PP} parameter of the other ECAPs.

Table 5.10 - More statistical data on V_{DC}/V_{PP} (value 0 also assigned when $V_{PP} = 0$)

	ECAP 1	ECAP 2	ECAP 3	ECAP 4
Mean	0.0815	0.1354	0.1663	0.1736
Minimum	-0.2232	-0.6246	-0.5164	-0.3566
Minimum of TOFs scored 'valid'	-0.2232	-0.4584	-0.5164	-0.3566
Maximum	3.1279	5.1469	1.6682	1.7276
Maximum of TOFs scored 'valid'	1.6834	2.1892	1.6682	1.7276

5.3 Latency related parameters of single ECAPs

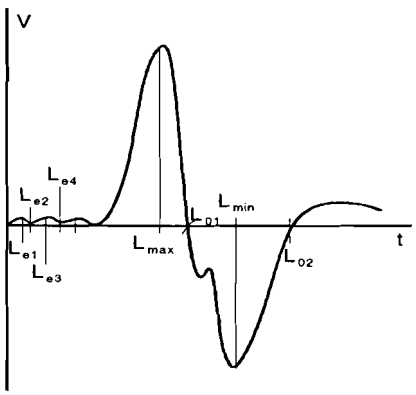

Figure 5.12 - Parameters related to the latency of extrema

Latencies of several peaks (see figure 5.12) were calculated. If a peak was not present , the latency was attributed the value -2 ms to be able to distinguish this case in the histograms. Of course the latencies of the minimum and maximum peaks were found in every ECAP.

5.3.1 Latencies of maximum peaks

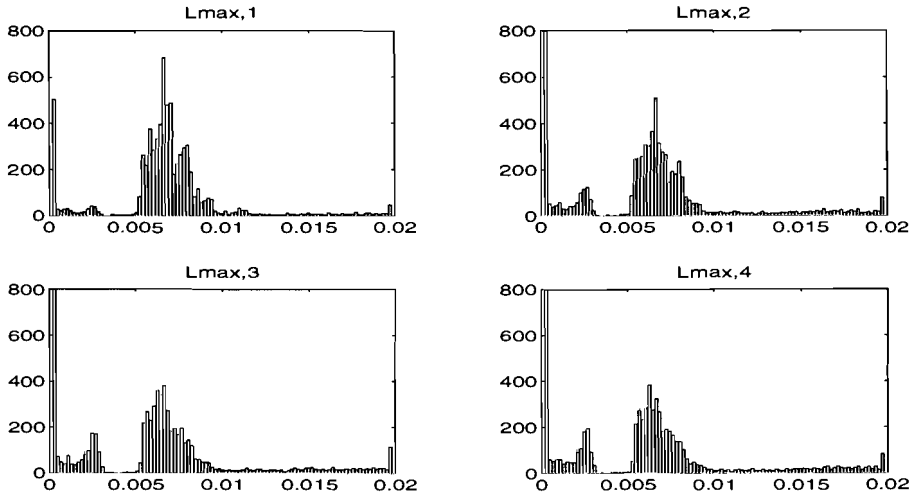

Figure 5.13 - Histograms of the latency (in s after stimulation) of the maximum peak of ECAPs 1 to 4. The maximum bin heights are 684, 841, 1071 and 1164, respectively. The average value 6.4 ms, standard deviation 4.3 ms.

The histograms in figure 5.13 show that most of the maximum peaks occur in the 5-10 ms interval. As table 5.12 shows, 'valid' TOFs have LMAX values ranging from the absolute minimum (0 ms) to the maximum (20 ms), so it seems that this parameter is at least not decisive for the validation. However, when inspecting the percentage of 'invalid' TOFs as a function of LMAX (figure 5.14), one finds that very small values (almost zero), caused the TOF to be invalidated in circa 40% of the cases.1

Table 5.11 - More statistical data on LMAX (values in ms after stimulus)

	ECAP 1	ECAP 2	ECAP 3	ECAP 4
Mean	6.70	6.41	6.21	6.08
Minimum	0	0	0	0
Minimum of TOFs scored 'valid'	0	0	0	0
Maximum	20	20	20	20
Maximum of TOFs scored 'valid'	20	20	20	20

In table 5.12, it may be seen that the average LMAX decreases for every ECAP of a TOF. This is remarkable. Although the latency shift is small, it is consistent. No explanation of this fact has been found yet.

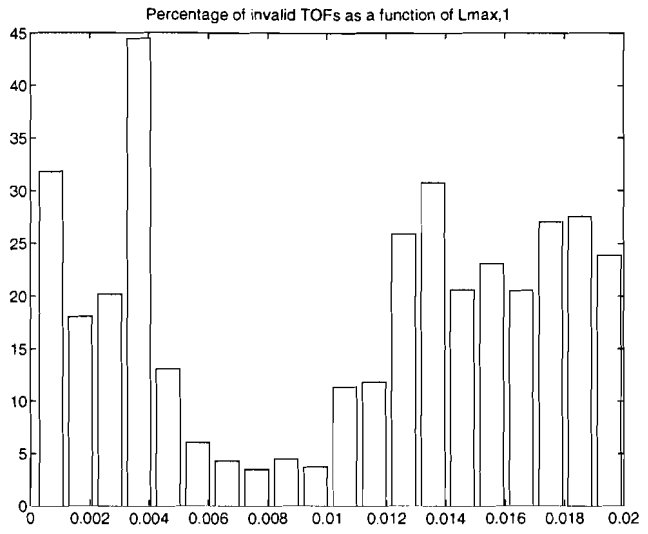

Figure 5.14 - Percentage of 'invalid' TOFs as a function of LMAX of the first ECAP

Figure 5.15 shows the latencies of the minimum. The histograms clearly show two distinct peaks: a sharp one at 5 ms and a more rounded one at circa 12 ms. Inspection of the ECAPs with minima at 5 ms showed that these minima appeared in cases of direct stimulation of the muscles, and in cases of high relaxation levels. At low levels of relaxation, the amplitude of the 12 ms negative peak is much larger than the amplitude of the peak at 5 ms, so the latency of the minimum is 12 ms. When relaxation increases, the 12 ms peak practically disappears, but the 5 ms peak remains present, so the latency of the minimum becomes 5 ms.
This means that an LMIN value of 5 ms may be valid or may indicate direct stimulation. The 12 ms minimum most often indicates lower levels of relaxation.

5.3.2 Latencies of minimum peaks

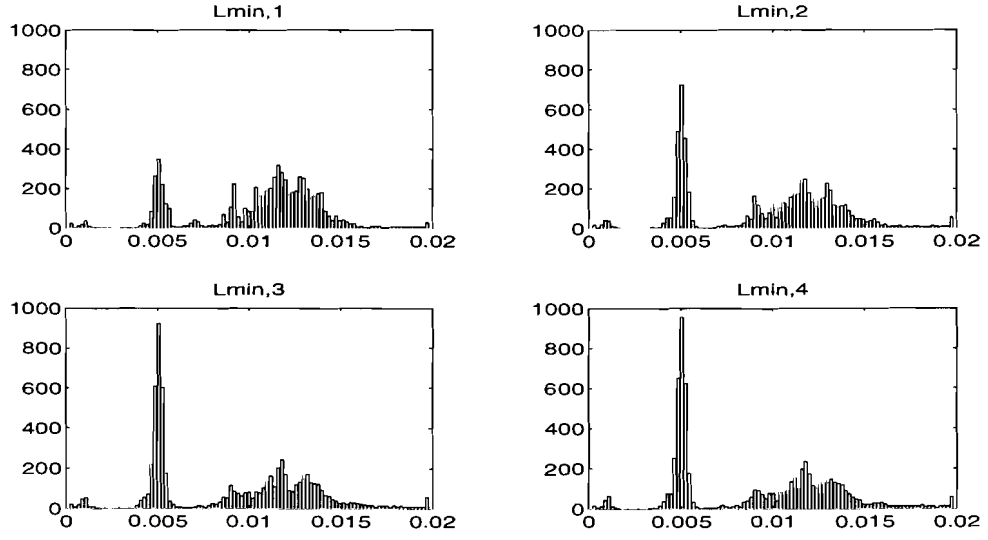

Figure 5.15 - Histograms of the latency of the minimum peak (in s after stimulus)

Table 5.12 - More statistical data on LMIN (values in ms)

	ECAP 1	ECAP 2	ECAP 3	ECAP 4
Mean	10.54	9.62	9.04	8.95
Minimum	0	0	0	0
Minimum of TOFs scored 'valid'	0	0	0	0
Maximum	20	20	20	20
Maximum of TOFs scored 'valid'	20	20	20	20

From the above and from table 5.13 it may be concluded that the only suitable LMIN criterium would be that if it is smaller than about 1 ms, the ECAP is probably invalid.
Finally, note that the mean LMIN values show the same decreasing trend as the mean LMAX.

5.3.3 Delay between minimum and maximum peaks

During the manual validation (see chapter 6), the time delay between the minimum and maximum peaks did not seem to vary much, so it could be a good indicator for the validity of the signal. Figure 5.16 shows the results, and table 5.14 shows more statistical data.
By definition, the mean of LMIN - LMAX is equal to the difference of their respective means.
The mean value of this parameter shows a slightly decreasing trend over the four ECAPs, just like the LMIN and LMAX values themselves. It seemed that the mean ratio of LMAX / LMIN was constant for all four ECAPs (0.667, standard deviation 0.023), so the response seemed to be 'scaled' in time. No further explanation for this could be found.

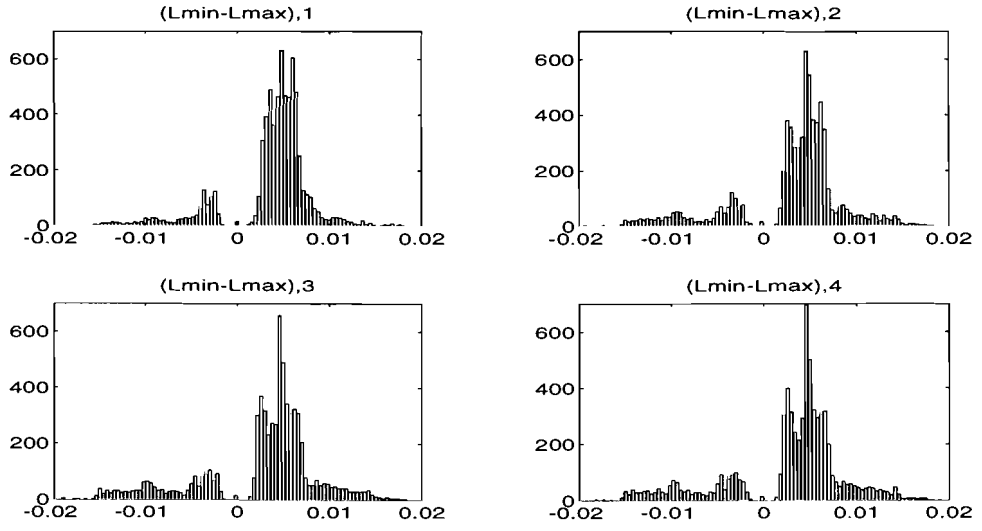

Figure 5.16 - Histograms of LMIN - LMAX (values in s). The average value is 3.2 ms, and the standard deviation is 5.7 ms.

Table 5.13 - More statistical data on LMIN - LMAX (values in ms)

	ECAP 1	ECAP 2	ECAP 3	ECAP 4
Mean	3.84	3.21	2.83	2.87
Minimum	-19.0	-19.6	-19.2	-18.4
Minimum of TOFs scored 'valid'	-19.0	-19.2	-18.8	-18.4
Maximum	18.4	19.2	18.4	19.2
Maximum of TOFs scored 'valid'	17.8	19.2	18.4	19.2

5.3.4 Latencies of zero crossings

A zero crossing detection algorithm was designed to detect if and where zero crossings occurred in each ECAP. The algorithm scans all samples of the ECAP in time order. A zero crossing was then defined to occur if the sign of the current sample is opposite to the sign of the last non-zero sample.

The index n_{zc} of the sample to which a crossing was attributed was calculated as follows:

$$n_{zc} = n_b + \text{round}[\ (n_b + n_a) / 2\ ],$$

where n_b is the index of the last non-zero element before the crossing, n_a is the first non-zero element after the crossing, and round(x) is the integer number nearest to x.

In this way, it was possible to study the number and latencies of the zero crossings.

The latency of the first zero crossing is shown in 5.17.

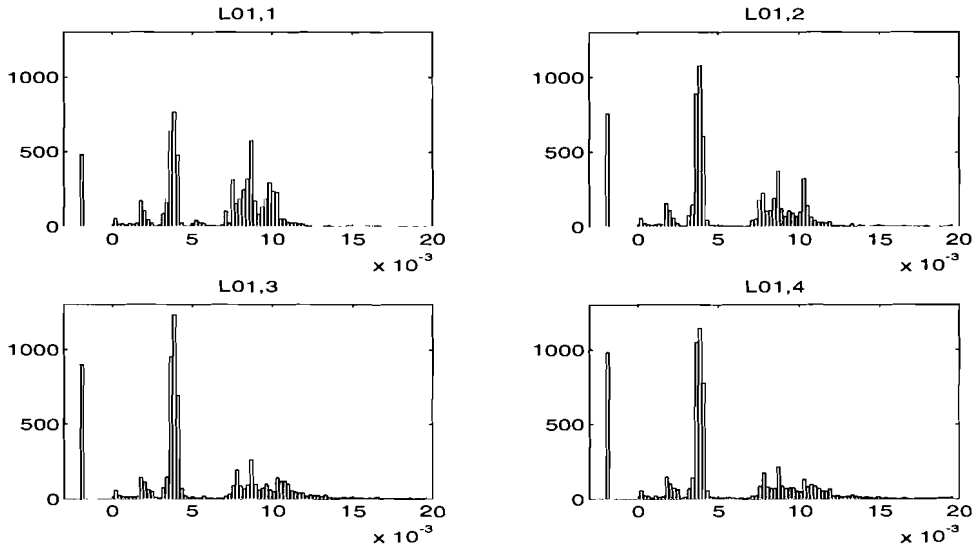

Figure 5.17 - Histograms of the latency of the first zero crossing (L_{01}, in s). The value -2 ms was assigned if no zero crossing was found.

Table 5.14 - More statistical data on L_{01} (values in ms). The value -2 ms was assigned if no zero crossing was found.

	ECAP 1	ECAP 2	ECAP 3	ECAP 4
Mean	6.0	5.2	4.8	4.7
Minimum	-2.0	-2.0	-2.0	-2.0
Minimum of TOFs scored 'valid'	-2.0	-2.0	-2.0	-2.0
Maximum	20	20	20	20
Maximum of TOFs scored 'valid'	20	20	20	20

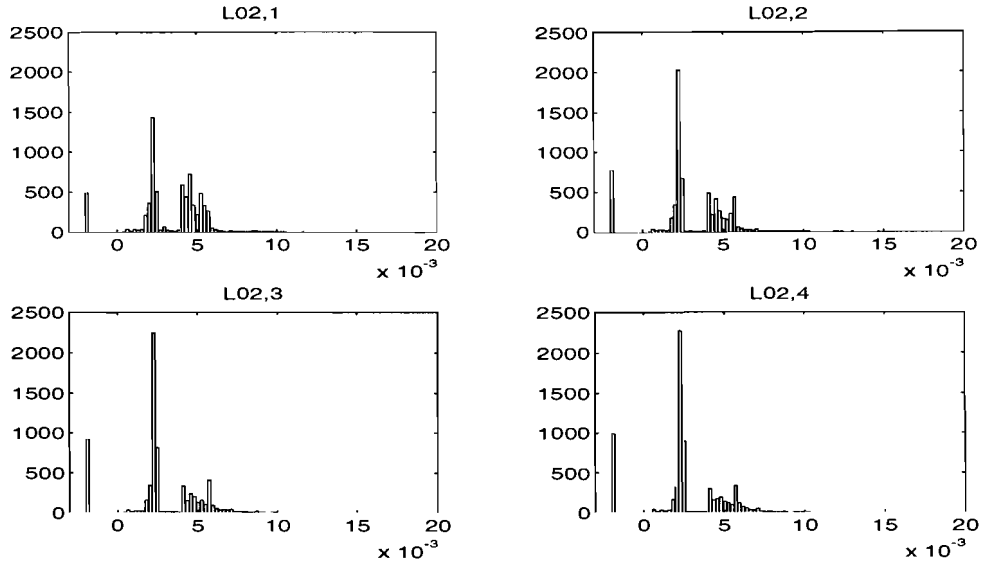

Figure 5.18 - Histograms of the latency of the second zero crossing (L_{02}, in s). The value -2 ms was assigned if no zero crossing was found. Mean value 2.8 ms, standard deviation 2.3 ms.

Table 5.15- More statistical data on L_{02} (values in ms after stimulus). The value -2 ms was assigned if no zero crossing was found.

	ECAP 1	ECAP 2	ECAP 3	ECAP 4
Mean	3.3	2.9	2.6	2.5
Minimum	-2	-2	-2	-2
Minimum of TOFs scored 'valid'	-2	-2	-2	-2
Maximum	17.4	18.8	18.8	14.8
Maximum of TOFs scored 'valid'	17.4	18.8	18.8	11.0

5.3.5 Number of zero crossings

The results of a count of zero crossings in every ECAP over all measured TOFs are shown in figure 5.19. Zero crossing counts of over five did not occur too often, although some of them were valid. Figure 5.20 shows the percentage of TOFs that was judged 'invalid' by hand, as a function of N_0 of the first ECAP of every TOF. From this figure it is clear that as the number of zero-crossings increases, the signal quality decreases. This is obvious since noisier signals are small, have many fluctuations around zero, so they will contain more zero crossings.

Table 5.16- More statistical data on N_0 in all ECAPs.

	ECAP 1	ECAP 2	ECAP 3	ECAP 4
Mean	2.53	2.50	2.48	2.45
Minimum	0	0	0	0
Minimum of TOFs scored 'valid'	0	0	0	0
Maximum	11	10	13	11
Maximum of TOFs scored 'valid'	9	10	13	11

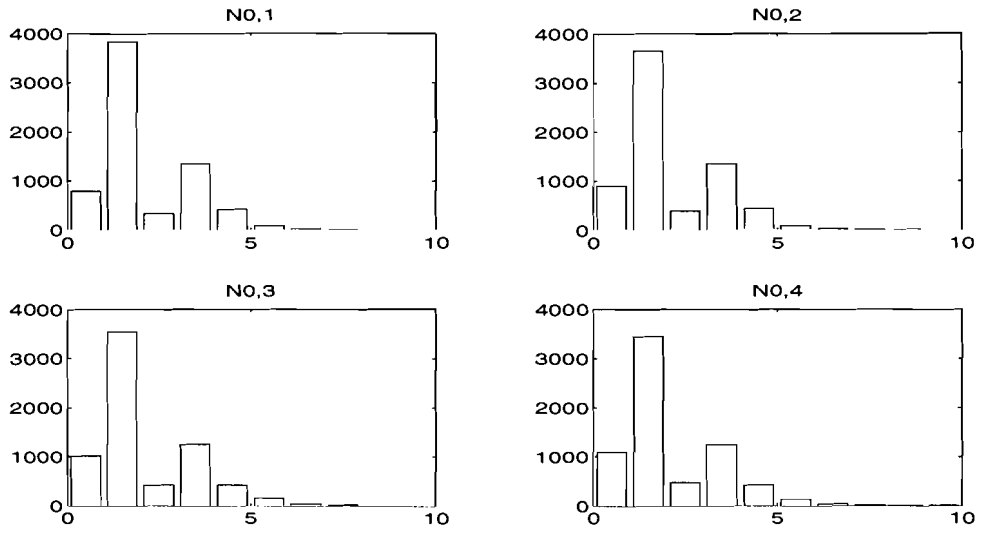

Figure 5.19 - Histograms of the number of zero-crossings. Average = 2.49 crossings, standard deviation = 1.47.

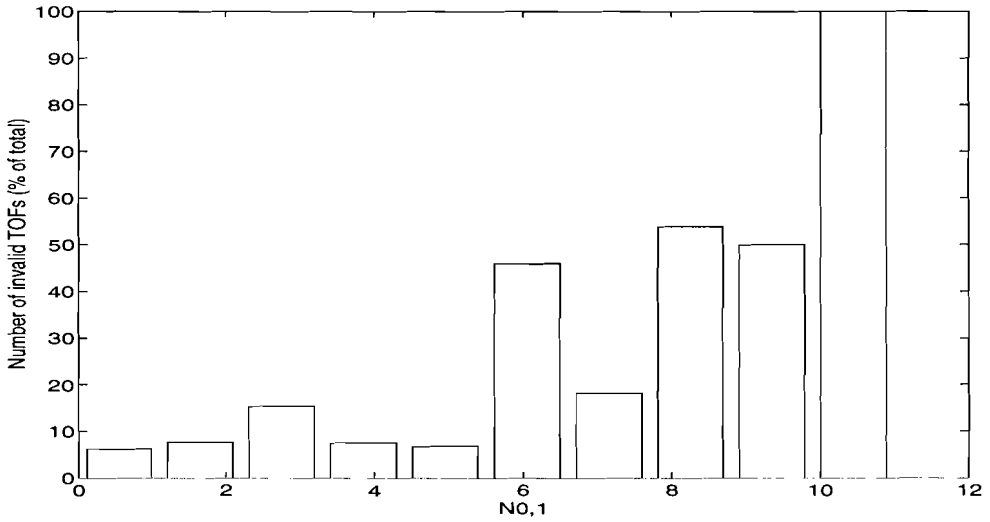

Figure 5.20 - Number of 'invalid' TOFs as a percentage of all TOFs, as a function of the number of zero crossings in the first ECAP of the measured TOFs.

5.3.6 Irregularity parameter

In 1995 Zalewska and Hausmanowa-Petrusewicz proposed a new measure to quantify the irregularity of single motor unit action potentials [Zalewska 1995]. We will apply it to the evoked compound action potential. It is defined as follows:

$$\text{If } V_{PP} > 0, \text{ then } C_{irr} = \frac{1}{V_{pp}} \sum_{i=1}^{n_s-1} |y_{i+1} - y_i| \ ,$$

else $C_{irr} = 2$,

where V_{PP} is the peak-peak amplitude, y_i is the sample with index i, and n_s is the number of samples. The measure actually depends on the 'length' of the ECAP curve. This length increases

as the ECAP becomes more irregular. C_{irr} is independent of the amplitude and duration of the peak. By definition, it has the following properties:

1. For a 'normal' biphasic action potential, with positive and negative peaks *a* and *-b*, (a > 0, b > 0), C_{irr} is equal to:

$$C_{irr} = (2a + 2b) / (a + b) = 2.$$

2. For a multiphasic signal with n_p positive and n_n negative peaks all with the same absolute amplitude *a*, C_{irr} is equal to:

$$C_{irr} = (2n_p a + 2n_n a) / 2a = n_p + n_n = n\,,$$

which is the number of phases.

3. For a signal with small amplitude fluctuation (local extrema) superposed on the signal, it can be shown that C_{irr} is equal to $4\,a\,N_{LE} / A$, where *a* is the peak-peak amplitude of the fluctuation, N_{LE} is the number of local extrema and *A* is the peak-peak amplitude of the signal. This means that for this type of signals, Cirr is proportional to the number of turns, but multiplied by their 'significance'. That is why a number of small turns will not alter the irregularity of the signal.

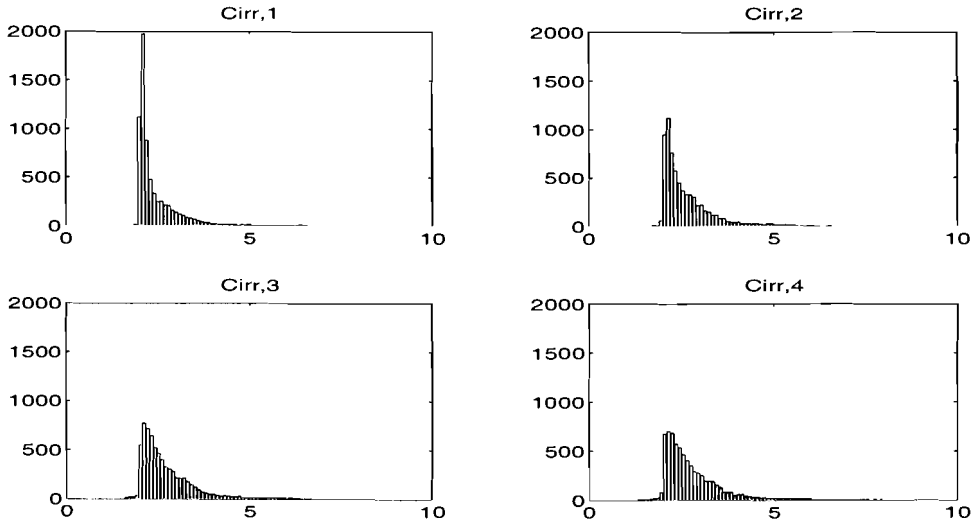

Figure 5.21 - Histograms of the irregularity parameter (C_{irr}) for all four ECAPs. The mean value is 2.643, with a standard deviation of 0.789.

Some signals were not measured correctly, and had a V_{PP} equal to zero. These were attributed a C_{irr} value of 2, since $\lim_{V_{pp} \downarrow 0} C_{irr} = 2$. Figure 5.21 shows the histograms of the resulting C_{irr} of all four ECAPs.

Table 5.17- More statistical data on C_{irr}. A value of -1 means that V_{PP} for the given measurement was equal to 0.

	ECAP 1	ECAP 2	ECAP 3	ECAP 4
Mean	2.464	2.634	2.726	2.747
Minimum	2.0	2.0	2.0	2.0
Minimum of TOFs scored 'valid'	2.0	2.0	2.0	2.0
Maximum	10.27	12.00	10.50	8.046
Maximum of TOFs scored 'valid'	9.300	10.70	9.500	8.046

As could be expected from the visual inspection, C_{irr} increases in every ECAP of a TOF, because the second, third and fourth ECAPs decrease in amplitude, and become more like a noisy signal.

5.4 Change of parameters within single TOFs

In this paragraph we will focus on the change in ECAP parameters within one train of four.

5.4.1 Change of T in a TOF

From visual inspection it was clear that the shape of undisturbed ECAPs of all four twitches was almost equal, except for the amplitude. The amplitude of the four twitches decreases exponentially, due to muscle fatigue. With low levels of relaxation, the fade is minimal. It increases with higher levels of relaxation. The difference $ECAP_n$ - $ECAP_{n-1}$ is therefore expected to be negative most of the time.

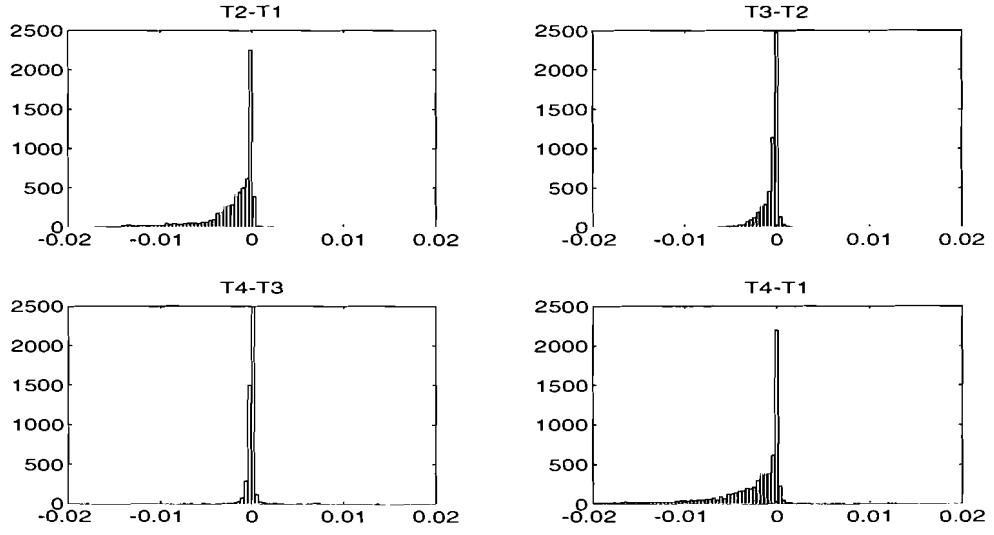

Figure 5.22 - Histograms of the difference between the T parameter between two ECAPs of the same TOF. Overall mean = -1.3 mVs, standard deviation 2.9mVs.

Table 5.18- More statistical data on T_n - T_{n-1}. (values in mVs).

	$T_2 - T_1$	$T_3 - T_2$	$T_4 - T_3$
Mean	-2.06	-0.442	-0.0874
Minimum	-21.1	-9.00	-0.0805
Minimum of TOFs scored 'valid'	-21.1	-9.00	-76.9
Maximum	42.0	63.3	14.0
Maximum of TOFs scored 'valid'	11.8	63.3	7.02

5.4.2 Change of N_0 in a TOF

The change in the number of zero crossings within normal TOFs is only small. Although valid measurements exist with NO_n - NO_m over the whole range from minimum to maximum, the larger values were in many cases associated with artefacts. Therefore this parameter seems to be suitable for validation.

Table 5.19- More statistical data on NO_n - NO_{n-1}..

	NO_2 - NO_1	NO_3 - NO_2	NO_4 - NO_3
Mean	-0.0315	-0.0243	-0.0273
Minimum	-8	-9	-9
Minimum of TOFs scored 'valid'	-8	-9	-9
Maximum	9	9	6
Maximum of TOFs scored 'valid'	9	9	6

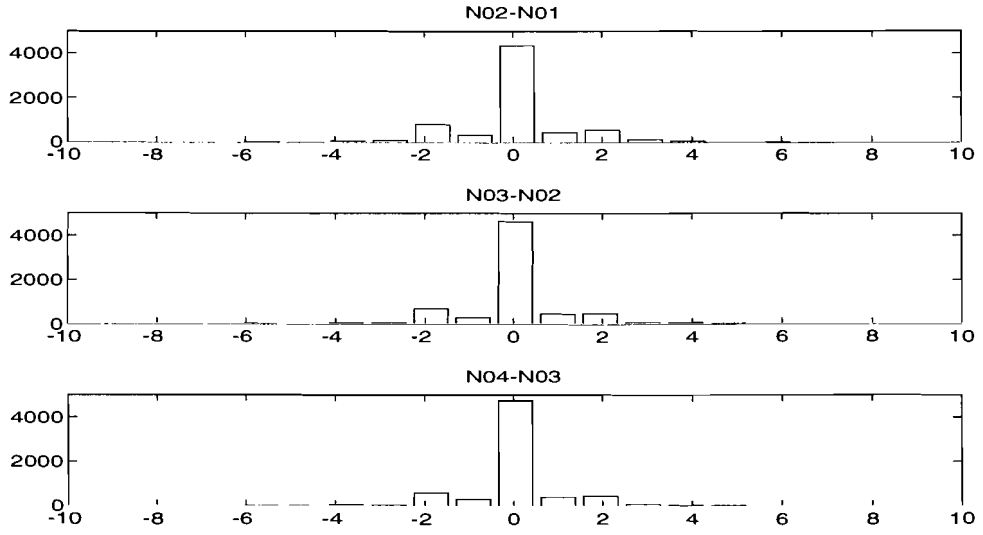

Figure 5.23 - Histograms of the difference in zero crossing counts between two ECAPs of the same TOF. Mean = -0.0277, standard deviation = 1.223.

5.4.3 Change of C_{irr} in a TOF

The histograms show that C_{irr} more often increases than decreases during a TOF. This could already be seen in figure 5.21.

Table 5.20 - More statistical data on $C_{irr,n}$ - $C_{irr,n-1}$.

	$C_{irr,2}$-$C_{irr,1}$	$C_{irr,3}$-$C_{irr,2}$	$C_{irr,4}$-$C_{irr,3}$
Mean	0.1701	0.0925	0.0199
Minimum	-6.4419	-9.6573	-6.2529
Minimum of TOFs scored 'valid'	-5.389	-8.342	-6.2529
Maximum	8.660	5.714	4.8985
Maximum of TOFs scored 'valid'	8.660	5.714	4.4988

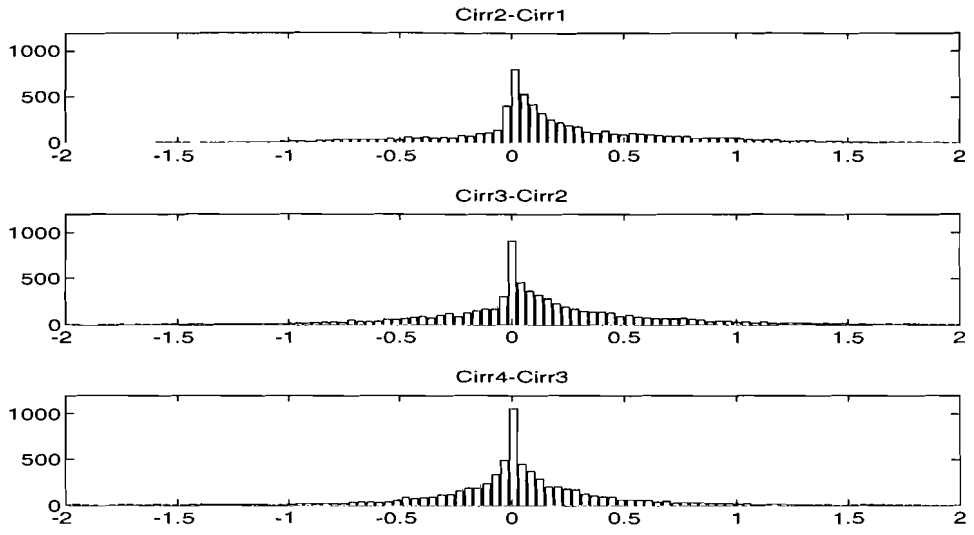

Figure 5.24 - Histograms of the difference in the irregularity parameter between two ECAPs of the same TOF. Mean = 0.0942, standard deviation = 0.608.

5.4.4 Change of V_{MAX}/T in a TOF

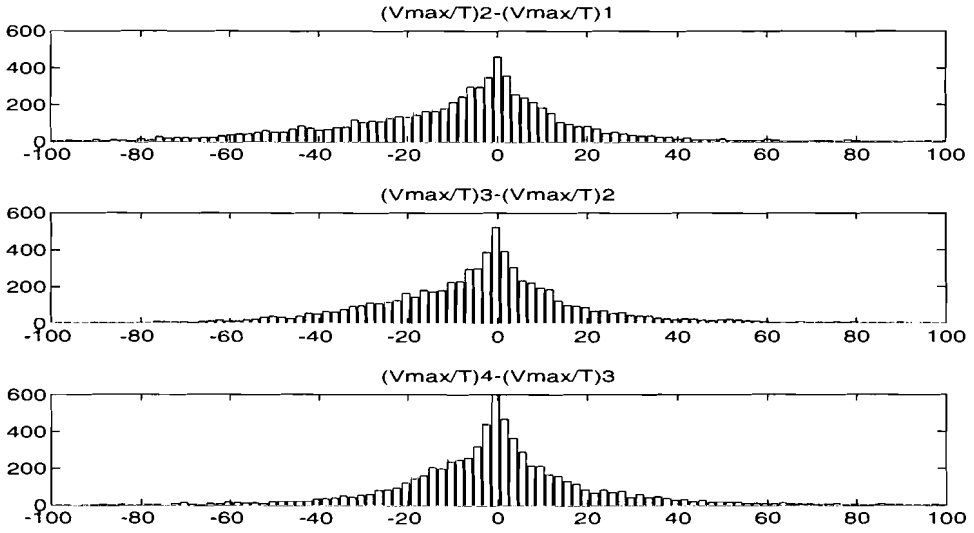

Figure 5.25 - Histograms of the difference in V_{MAX}/T between two ECAPs of the same TOF. Mean = -4.174, standard deviation = 31.21.

Values greater than 100 or smaller than -100 were often due to artefacts. This parameter seems to be suitable for validation purposes. Note that normal values for V_{MAX}/T range from 50 to 200 s^{-1}, so the relative change within each TOF is small.

Table 5.21 - More statistical data on $(V_{MAX}/T)_n - (V_{MAX}/T)_{n-1}$. Values are in s^{-1}.

	$(V_{MAX}/T)_2 - (V_{MAX}/T)_1$	$(V_{MAX}/T)_3 - (V_{MAX}/T)_2$	$(V_{MAX}/T)_4 - (V_{MAX}/T)_3$
Mean	-8.04	-3.76	-0.73
Minimum	-1207	-267.4	-225.5
Minimum of TOFs scored 'valid'	-139.0	-180.4	-190.0
Maximum	445.7	301.3	1250
Maximum of TOFs scored 'valid'	195.6	184.7	188.9

5.5 Change of parameters in successive TOFs

The change of several TOF parameters over time was studied. The parameters of a TOF were compared to those of the previous TOF that was considered valid by the algorithm. The difference of each parameter (e.g. V_{MAX}) that was calculated in this way, was assigned to a new parameter (e.g. ΔV_{MAX}). The new parameters have been analyzed like the previous parameters.
Since (in steady state) the controller should warn the clinician after circa 5 subsequent invalid measurements, the previous valid measurement will never be older than circa 2 minutes. For this analysis however, valid measurements older than 2 minutes were also compared to.

5.5.1 Change of T in successive TOFs

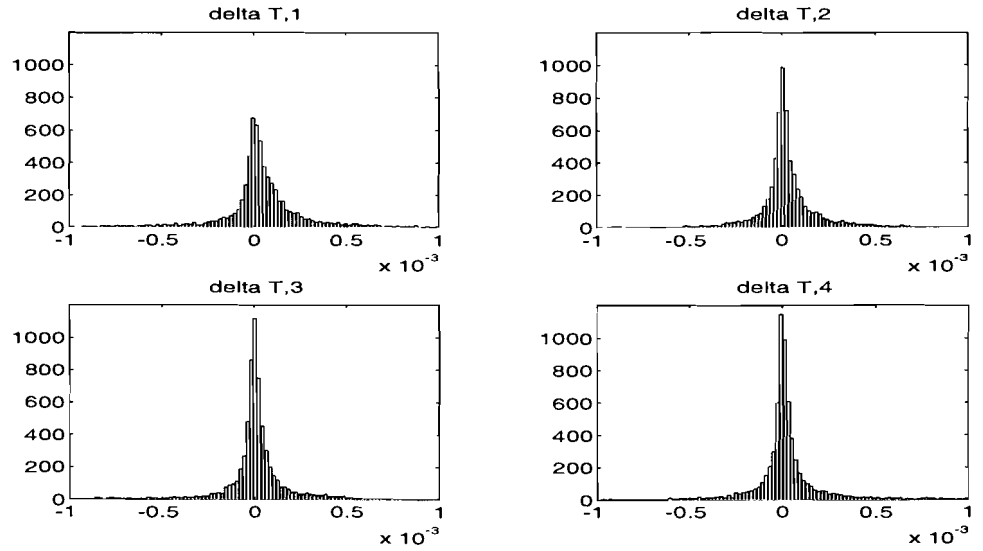

Figure 5.26- Histograms of the change in T between two ECAPs of successive TOFs. Over-all mean = -4.762 · 10⁻⁵ Vs, standard deviation = 1.5 · 10⁻³ Vs.

The histograms show that ΔT has a normal distribution, with the exception that there are a little more positive than negative values, because the increase of T (in the recovery phase) takes more time and is present in more measurements. The rapid decrease of T during the onset phase is reflected by a few large negative parameter values.
The high maximum of ΔT_3 (table 5.23) was caused by an artefact. Since it occurred in ECAP 3, the concerning TOF had not been scored 'valid'.

Table 5.22 - More statistical data on ΔT_n. All values are in Vs.

	ΔT_1	ΔT_2	ΔT_3	ΔT_4
Mean	$-0.4743 \cdot 10^{-4}$	$-0.4806 \cdot 10^{-4}$	$-0.3445 \cdot 10^{-4}$	$-0.6053 \cdot 10^{-4}$
Minimum	-0.0317	-0.0314	-0.0311	-0.0311
Minimum of TOFs scored 'valid'	-0.0232	-0.0211	-0.0211	-0.0212
Maximum	0.0217	0.0284	0.0750	0.0171
Maximum of TOFs scored 'valid'	0.0217	0.0143	0.0750	0.0138

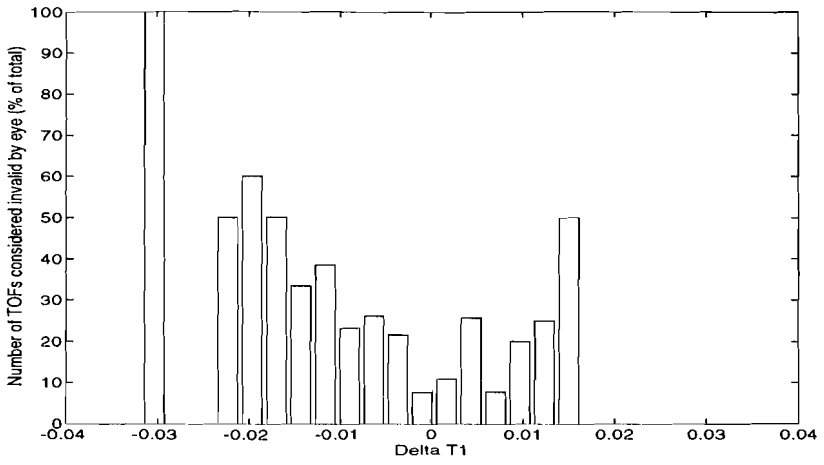

Figure 5.27 - Number of TOFs scored 'invalid' by eye as a percentage of all TOFs, as a function of the change of T_1 over successive TOFs.

5.5.2 Change of other parameters in successive TOFs

The distribution of the change in other parameters was comparable to that of T_1. These distributions were more or less gaussian. Table 5.24 shows a summary of these other parameters and their statistical properties.

Table 5.23 - Statistical data on the change of other parameters

Parameter	Property	TOF	ECAP 1	ECAP 2	ECAP 3	ECAP 4
ΔC_{irr}	Mean	0.0038	0.0034	0.0042	0.0046	0.0032
	Standard deviation	0.6214	0.6321	0.6386	0.6126	0.6019
	Minimum		-6.427	-9.116	-7.362	-7.362
	Minimum of TOFs scored 'valid'		-6.42	-7.667	-7.362	-5.705
	Maximum		8.218	9.882	7.333	5.680
	Maximum of TOFs scored 'valid'		6.985	8.453	7.333	5.416
ΔL_{MAX}	Mean	-9.85µs	-11.43 µs	-40.4 µs	-12.15 µs	-11.81 µs
	Standard deviation	5.2 ms	3.6 ms	5.2 ms	5.7 ms	5.8 ms
	Minimum	-20 ms	-20 ms	-20 ms	-20 ms	-20 ms
	Minimum of TOFs scored 'valid'	-20 ms	-20 ms	-20 ms	-20 ms	-20 ms
	Maximum	20 ms	20 ms	20 ms	20 ms	20 ms
	Maximum of TOFs scored 'valid'	20 ms	20 ms	20 ms	20 ms	20 ms
$\Delta N0$	Mean	-0.0138	-0.0135	-0.0128	-0.0148	-0.0141
	Standard deviation	1.201	1.079	1.154	1.253	1.307
	Minimum		-9	-8	-9	-9
	Minimum of TOFs scored 'valid'		-8	-8	-9	-9
	Maximum		9	8	9	10
	Maximum of TOFs scored 'valid'		7	8	9	8
ΔV_{DC1}	Mean	-132µV	-0.791mV	-0.140mV	0.815mV	-0.415mV
	Standard deviation	50.9mV	35.9 mV	42.9 mV	77.3 mV	35.6 mV
	Minimum		-0.814 V	-0.532 V	-0.628 V	-0.9051 V
	Minimum of TOFs scored 'valid'		-0.814 V	-0.532 V	-0.628 V	-0.9051 V
	Maximum		0.6765 V	2.629 V	4.568 V	0.8724 V
	Maximum of TOFs scored 'valid'		0.4756 V	0.5488 V	3.163 V	0.8724 V

5.6 Selection of parameters and bounds

From the above, it was clear that certain parameters (e.g. T, V_{PP}) depend mainly on the relaxation level, and are not very sensitive to artefacts. These parameters do not seem to be very suitable for validation. The only clear bounds that may be posed on them lie far from the mean value and are based on the technical limits of the measurement system. Some of these parameters were included however, to be able to detect errors that did not occur in the learning set and may not be noted by other parameters.
An other group of parameters is relatively independent on the relaxation level, and is more sensitive to artefacts. Certain values usually occur in valid TOFs, and more extreme values occur when artefacts are present. To these parameters, narrower bounds can be applied.

As discussed earlier, it was expected that parameters would have a more or less gaussian shape, with clearly visible outliers, caused by artefacts. However, in most histograms this distinction could not be made that easily, and the choice for the parameter bounds was not obvious. In these cases, the bounds were derived from the 'invalid percentage' diagrams. Such a diagram shows the number of measurements that was considered 'invalid' by visual inspection as a function of the parameter p. The number of measurements is expressed as a fraction of all measurements with the given parameter value.

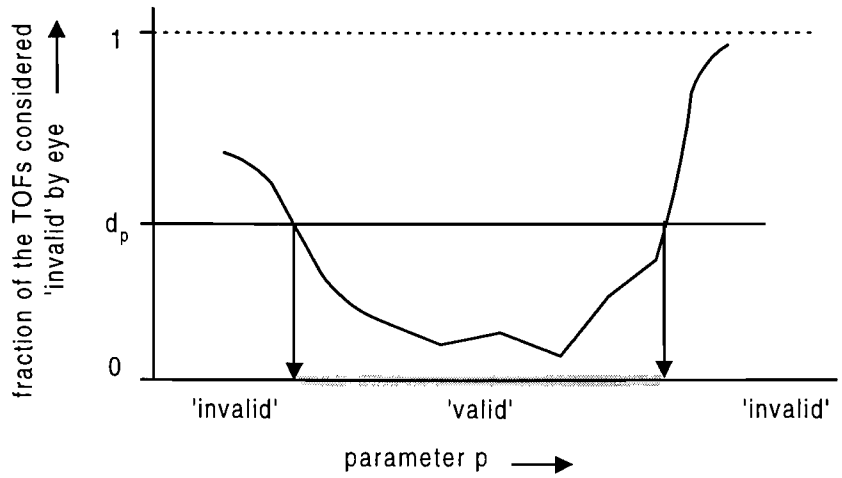

Figure 5.28 - Relationship between d_p and the range in which the algorithm will consider the signal valid.

If for a certain range of parameter values this fraction is higher than some threshold d_p ($0 < d_p < 1$), the validation algorithm should consider measurements in that range invalid. For the sake of simplicity, the criteria should be of the type '$p_{lower\ bound} < p < p_{upper\ bound}$' or '$p < p_{bound}$' or '$p > p_{bound}$'.

By varying d_p, the performance of the parameter may be tuned. High values for d_p will cause many invalid measurements to be let through, but the measurements that are called invalid, are sure to be unreliable. Low values make the algorithm more restrictive, so many valid measurements will be called invalid, but artefacts are discovered almost certainly.

It must be noted that d_P relates to the performance of one parameter only, and that the over-all performance of the validation algorithm will depend on the d_P s of all parameters.

As a compromise between the above extremes, it was decided to try $d_P = 0.50$ for all parameters.

The results of this procedure are shown in appendix B, which contains a list of all selected parameters and their bounds.

6. Results

The developed data acquisition system was tested in the operating rooms of the Catharina hospital. The goals of these measurements were to test the reliability and accuracy of the data acquisition system, and to acquire a set of TOF EMG signals to test the validation algorithm.
After informing the local medical ethical committee, NMT measurements of 18 patients were recorded using the NMT module of the AS/3 ADU. The EMG electrodes were placed according to figure 2.1. A total of 5129 measurements were collected.
After discussing the performance of the two data acquisition systems used for measuring the learning and test sets of data, the performance of the validation algorithm will be discussed.

6.1 Performance of the data acquisition systems

6.1.1 Accuracy of Relaxograph / Labmaster system

The learning set was measured using the Relaxograph NMT-100, combined with a Labmaster A/D board. The T parameter values as calculated by the PC have been compared to the Relaxograph's own measurements, sent over the serial link. Results are shown in figure 6.1 and figure 6.2.

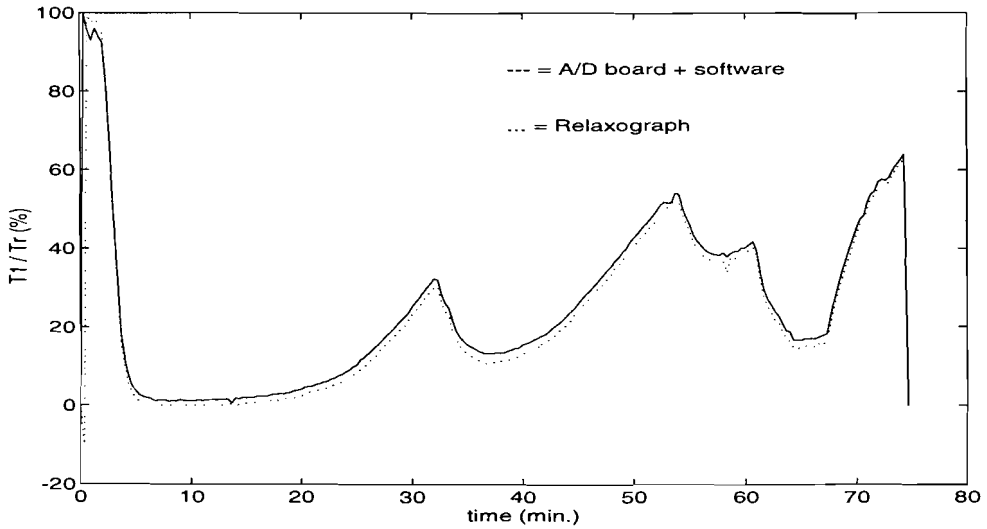

Figure 6.1 - T_1/T_{ref} calculated by the Relaxograph and by the PC measurement system.

When comparing the T_1/T_{ref} produced by the Relaxograph and by the PC, a minor difference is noted. Furthermore, the PC's measurements seem to react differently to disturbances (for example at the start and after 58 minutes). This may be due to some averaging algorithm in the Relaxograph's software.

Figure 6.2 shows the correlation between the two calculations. For this plot, the quantisation error of the Relaxograph may be noted at low T_1/T_{ref} levels. The mean absolute error was 3.38% of T_{ref}. Since the serial port of the AS/3 NMT was not used, this comparison cannot be made for the system which acquired the test set.

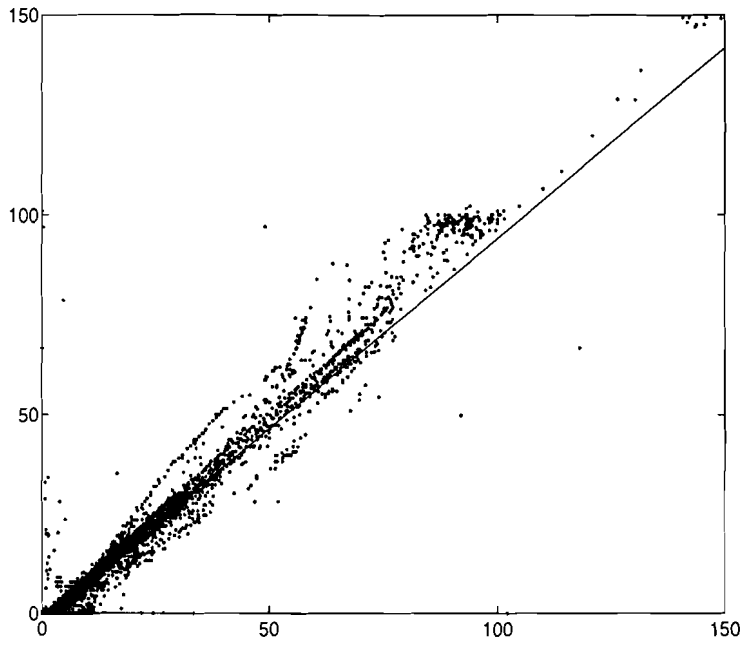

Figure 6.2 - Correlation between Relaxograph's and PC's relaxation measurements (uncalibrated measurements were excluded). Approximation: y = ax + b with a = 0.9534 and b = -1.2915 %. Vertical axis: T_1 / T_{ref} according to Relaxograph, horizontal: idem, according to PC.

6.1.2 Accuracy of AS/3 NMT module and PC

The final data acquisition system functioned stabily. Measurements were collected, shown on screen and stored on disk.

At the AS/3 output an offset voltage was observed. Since this voltage varied slightly over time, it had to be compensated for. The average of some of the first samples of each twitch was subtracted from the twitch. After applying this correction, the readings of T_1 / T_{ref} and T_4 / T_1 on both PC and AS/3 were comparable. Calibration of the AS/3 NMT module was successful in 17 of the 18 cases.

Compared to the measurements with the Relaxograph, the sensitivity of the system to electric interference by diathermia was considerably smaller. The amplitudes of artefacts were smaller. This is probably due to better grounding and shielding of the A/D board and connecting cables.

6.2 Performance of the validation algorithm

The validation criteria have been determined using a rather 'dirty' set. First the performance of the chosen parameters and criteria will be assessed. This is done by comparing the outcomes of validation with the algorithm against the 'ideal outcome' or 'golden standard'. This golden standard is set by an expert. Since it is not common practice to monitor evoked train-of-four EMG signals, such experts are hard to find. It was supposed that in this case, the validity could be judged by the author. In the next paragraphs the manual validation of the learning and test set will be discussed.

6.2.1 Goal of manual validation

The goal was to score which train-of-four responses would yield a T_1/T_{ref} measurement of a quality that is reliable enough to use for closed loop control. By doing this by eye, also a better insight might be gained in the shape of the responses and in which parameters could possibly be interesting candidates for the automatic validation algorithm.
The learning set as well as the test set have to be validated by eye. The learning set was recorded using the Relaxograph as an NMT device.

6.2.2 Method for validation by eye

Smans's measurement program EMG_MEAS.PAS was adapted to record and display validation information. The information was stored in a previously unused bit in the record structure of the measurement files. For each TOF, the bit was set when the TOF was scored 'invalid', and cleared if the TOF was scored 'valid'. The bit used is bit 3 of the 10th byte of the so called .serial field in the .TRF files. This byte is also used to store the three Relaxograph flags. The new coding is displayed in table 6.1.

Table 6.1 - New coding of the 10th byte of the .serial field in the .TRF files

Bit	Meaning
0 (LSB)	HF disturbance flag
1	electrodes off flag
2	uncalibrated mode flag
3	visual validation flag (0=valid, 1=invalid)
4-7	not used

The current state of the validation flag is displayed on the screen, and the user may toggle the flag on and off. An indication of the current position in the measurement file was also added.

As stated earlier, the main idea was that it would be better to discard measurements of which we doubted the quality, than to use a probably unreliable parameter as the control value. In the latter case the system could give the impression of good control while the controlled value had little or nothing to do with the muscle relaxation itself.

Since we wanted a rather strict validation, the following explicit rules of thumb have been used during the validation to make it more consequent:

- Measurements in which direct stimulation of the muscles was suspected should be discarded.
- The first twitch had to look well; if not, the measurement was considered invalid.
- If only the second, third or fourth twitch did not seem reliable, but the first one did, the measurement was called 'valid'.
- The quality of T_4 was more important than that of T_2 and T_3 because the T_4/T_1 ratio indicates the clinically important muscle fade, which is reliable only if T_4 is reliable.

6.2.3 Results of validation by eye

The quantitative results of the validation by eye are presented in table 6.2. The number of invalid measurements was lower in the test set. Because of the correct electrode placement, no direct stimulation was observed in the test set.

Direct stimulation was recognized due to its exponentially shaped, unipolar twitches, that also showed up at times the relaxation was sure to be 100%. These twitches showed no fade; the 4th of a TOF was as strong as the 1st. (They occurred most clearly in the M09.TRF file.)

The EMG response shape changes gradually as relaxation deepens. Especially the number of peaks seemed to increase when relaxation increased. The EMG signals during deeper levels of relaxation show relatively large variations in amplitude, but the number and place of the (small) maxima and minima seem to stay constant. The validation of these small signals proved to be more difficult, and a little more arbritrary than the larger and clearer signals.

Table 6.2 - Results of the validation by eye for the learning set and for the test set

	Considered 'valid' by eye	Considered 'invalid' by eye	Total
Learning set	6297 (91.5% of learning set)	581 (8.5% of learning set)	6878
Test set	4975 (97.0% of test set)	154 (3.0% of test set)	5129
Total	11272	735	12007

6.2.4 Results of automatic validation

The limits mentioned in chapter 5 were applied to the signals of the learning set. The results were compared to the 'golden standard' set by manual validation 'by eye' (table 6.3).

Table 6.3 - Performance of the validation algorithm on the learning set, compared to the 'manual inspection' by eye. In the columns the results of the validation by the algorithm are shown, while the rows show the outcome of the validation by eye.

By eye: \ Automatic:	Valid	Invalid	Total
Valid	4081	2216	6297
Invalid	76	505	581
Total	4157	2721	6878

- The algorithm detected 86.9% of all artefacts.
- The algorithm considered 64.8% of the measurements valid.
- In 66.7% of the cases the algorithm agreed with the inspection by eye.

The same criteria were applied to the test set as to the learning set as much as possible. The voltage related criteria were changed to fit the -5...+5V voltage range of the AS/3 ADU. The calculation of the parameters for the test set was adapted to the other time window and sample frequency.
The results were again compared to the manual validation. The performance of the algorithm on the test set is shown in table 6.4.

6.3 Discussion

Because of small differences between the test set and the learning set, the algorithm considers more measurements invalid in the test set than in the learning set. This appeared to be mainly due to the $N_{0,n}$ parameter (number of zero crossings of ECAP n in a TOF). The measurements of the learning set contained a small offset voltage that was enough to shift low signals completely above the 0V level. In the test set, this offset voltage was compensated for, so the number of zero crossings in small signals was higher.

Table 6.4 - Performance of the validation algorithm on the test set, compared to the inspection by eye. In the columns the results of the validation by the algorithm are shown, while the rows show the outcome of the validation by eye.

Automatic: / By eye:	Valid	Invalid	Total
Valid	1419	3556	4975
Invalid	23	131	154
Total	1442	3687	5129

- The algorithm detected 85.0% of all artefacts.
- The algorithm considered 28.1% of the measurements valid.
- In 30.2% of the cases the algorithm decided in accordance with the inspection by eye .

The percentage of measurements that were considered invalid by eye was smaller in the test set (3.0%) than in the learning set (8.5%). This improvement is probably due to the better electrode placement and to better shielding of the connecting wires. It may also be due to some (unknown) form of signal processing by the AS/3 monitor.

The number of measurements that were considered valid by the algorithm (28.1%) was on the bounds of the acceptable range (a minimum of circa 1 valid measurement every minute) for the steady state phase. Since the 'invalid' measurements are not evenly distributed, sometimes longer periods without valid measurements will occur, that may interrupt the controller operation.

The algorithm correctly identified 85% of the artefacts in the test set, which is close to the performance of the algorithm on the learning set. However, it is not 100%. This may be due to several reasons:

- Inaccurate validation by eye. As mentioned before, it was especially difficult to judge small noise-like signals. The noise on the signal made it difficult to discern the muscles response. A great deal of the time, the signals were small.
- During the manual validation, implicit rules of thumb may have been used. However, if these rules were a little fuzzy, and were not applied very consequently (which is typical for human 'experts'), it is difficult to 'reconstruct' them by a global statistical analysis of the data. So these 'fuzzy' rules could not be implemented in the algorithm.
- The selection of the parameters may not have been optimal. Including or excluding a parameter from the algorithm may change the number of correctly recognized artefacts, but also changes the number of incorrectly invalidated measurements. A good balance should be found when choosing parameters.

- Even if a 'sufficient' set of parameters was used, the choice of the criteria for these parameters influences the final validation performance. This is due to the smooth transition from the range of 'valid' parameter values to the range of 'invalid' values, that occurs for most parameters.

(Of course for all these causes, remedies may be sought.)

7. Conclusions and recommendations

7.1 Conclusions

7.1.1 Data acquisition system

A PC based data acquisition system for the acquiring of train-of-four EMG measurements has been constructed, that is suitable for linking with both the Datex Relaxograph NMT-100 and with the Datex AS/3 anaesthesia depth unit (ADU). During clinical trials with the ADU, the total system performance was satisfactory. Because of the use of an 'optimal' electrode positioning and because of better shielding and grounding, a reduction of the number of measurements with artefacts compared to a previous study was reduced from 8.5% to 3.0%.

7.1.2 Validation algorithm

A heuristic method for finding a validation algorithm for train-of-four muscle relaxation measurements was proposed, implemented and tested on clinical data.
A number of parameters was analyzed. Many signal parameters depend strongly on the level of muscle relaxation. A validation algorithm should cope with these large variations. The change in many parameters seemed to be limited.

A learning set and a test set of measurements were validated by visual inspection. It proved difficult to judge the small noise like signals in case of deep levels of relaxation.

The algorithm recognized circa 85% of the artefactual measurements. Based on the fact that a real optimization of the algorithm has not yet been carried out, better results are probably possible.

7.2 Recommendations

The performance of the validation algorithm may be optimized in several ways:

- The validation by visual inspection should be verified by reviewing the measurements or by comparing the current validation by eye to a second opininion. Was it consistent enough? Are there more rules or parameters that can be derived from the visual inspection?
- Search for 'better' parameters. The parameters used in this study were relatively simple, without or with only a simple compensation for the influence of the level of muscle relaxation. If the complex relationship between signal parameters and the level of muscle relaxation is modelled better, this may yield parameters that are better usable for validation.
- It could be interesting to see if an adapted form of the 'map' method by de Graaf [de Graaf 1993] can be used. A parameter that is the result of this method may be added to the existing algorithm.
- Search for better threshold values. By shifting the threshold values (or d_p), the performance of parameters may be tuned. Perhaps a machine learning program could be used to find an optimal set of thresholds.

When the validation algorithm functions properly, the design of the controller should be assessed.

- The use of a model predictive controller [Schwilden, Olkkola] seems promising in terms of accuracy and robustness. The advantage of using a model based (predictive) controller is that it is possible to specify future setpoints. This allows, for example, that the clinician specifies in advance that the patient should recover within 20 minutes. The controller may then

immediately adapt the infusion scheme, in order to reach the target level in time. Furthermore, if a model of the patient's muscle relaxation is available, and the parameters are adapted on-line, it may be possible to predict the time that is needed for spontaneous recovery at the end of the operation. This may help to determine the moment when infusion of muscle relaxants should be stopped.

- During the clinical trials, it was observed that the capnogram (expiratory CO_2 level as a function of time) was used by the clinicians to detect spontaneous breathing activity. Since spontaneous breathing may be a sign of insufficient muscle relaxation, it could be interesting to see if and how this signal can be used to improve the controller performance.

8. References

Blom JA, The SIMPLEXYS experiment, Real time expert systems in patient monitoring. Eindhoven: Eindhoven Technical University, 1990. Dissertation.

DAS-1600/1400 Series user's guide
Rev. B, 1996, Keithley Instruments, Inc., 440 Myles Standish Blvd. Taunton, MA 02780

DAS-1600/1400/1200 Series Function Call Driver User's Guide
Rev. B, 1995, Keithley Instruments, Inc., 440 Myles Standish Blvd. Taunton, MA 02780

de Graaf PMA,
Datareductie als basis voor validatie van fysiologische signalen. Graduation report TUE 1993

Metingen in de geneeskunde I,
Various authors, Reader TUE

Feldman S,
Neuromuscular block. Butterworth-Heinemann, Oxford 1996

Franklin, Gene F., Powell, J. David, Emami-Naeini, Abbas,
Feedback control of dynamic systems. Addison-Wesley 1994

Hines A.E., Crago P.E., Chapman G.J., Billian C.,
Stimulus artifact removal in EMG from muscles adjacent to stimulated muscles, in J. NEUROSCI. METHODS 1996 64/1 (p. 55-62).

Hoevenaren W.M.,
Ontwikkeling van een feedback controller voor spierrelaxatie met behulp van een expert-systeem (meetaspecten); afstudeerverslag TUE 1992

Hoogendoorn, Paul,
The design of a rule based blood pressure controller. Graduation report TUE 1989

Kalli, Illka,
Monitoring of neuromuscular blockade by electromyography with special reference to clinical application in anaesthetized infants and children. Diss. Helsinki University 1991.

Kirkegaard-Nielsen H., Helbo-Hansen H.S., Lindholm P. et al.,
Double burst monitoring during surgical degrees of neuromuscular blockade: A comparison with train-of-four. In: INT. J. CLIN. MONIT. COMPUT. 1995 12/4 (p. 191-196).

Knuttgen D., Burgwinkel W., Zur Nieden K. et al.,
Limited applicability of the Datex Relaxograph in diabetics with peripheral polyneuropathy; INT. J. CLIN. MONIT. COMPUT. 1996 13/1 (p. 21-25)

Mason DG, Linkens DA, Edwards ND, Reilly CS, Automated delivery of muscle relaxants using fuzzy logic control, IEEE Engineering in Medicine and Biology 1994; 13 : 678-686
Mason D.G. et al.,
Self-learning fuzzy control of atracurium-induced neuromuscular block during surgery. Medical & Biological Engineering & Computing 1997 35 (p. 498-503)

Melissen, Martin,
Een algemene methode van extractie en validatie van signaalparameters van biomedische signalen; Eindhoven University of Technology 1993. Graduation report.

Nikkelen A.L.J.M.,
Pharmacokinetic and pharmacodynamic modeling of neuromuscular blocking agents for educational simulation; Eindhoven : Technische Universiteit Eindhoven, 1995. Graduation report.

NMT-100 Technical Manual,
No. 870378-2, 1985, Datex Instrumentarium Corp., P.O. box 357, 00101 Helsinki 10, Finland.

Rowaan C.J. e.a.,
A complete and comprehensive computer-controlled neuromuscular transmission measurement system developed for clinical research on muscle relaxants. In J. CLIN. MONIT. 1993 9/1 (p. 38-44)

Scheepers F.N.L.H.,
Ontwikkeling van een regelaar voor spierrelaxatie met behulp van een expert-systeem (regelaspecten); afstudeerverslag TUE 1992

Schippers Houkje C.,
Pharmacodynamics of vecuronium bromide in anaesthetized neonates, infants and children. Proefschrift Erasmus Universiteit Rotterdam, Rotterdam 1988.

Smans J.L.A.,
Betrouwbaar meten van spierverslapping; afstudeerverslag TUE 1993

Smans J.L.A., Korsten H.H.M., en Blom J.A.,
Optimal surface electrode positioning for reliable train of four muscle relaxation monitoring; in International Journal of Clinical Monitoring and Computing 13: 9-20, 1996 Kluwer Academic Publishers

Van den Brom R.H.G.,
Monitoring of neuromuscular transmission with special emphasis on the assesment of intubating conditions. Groningen: Rijksuniversiteit Groningen, 1994. Dissertation.

Young, Shuenn-Tsong en Kuang-Ning Hsiao,
A pharmacokinetic model to study administration of intravenous anaesthetic agents; in IEEE Engineering in Medicine and Biology 1994, p. 263-268.

Zwart R.M.P.,

Appendix A: Wiring of PC - NMT monitor links

Link from Datex AS/3 ADU
to PC with Keithley DAS-1402 A/D conversion board

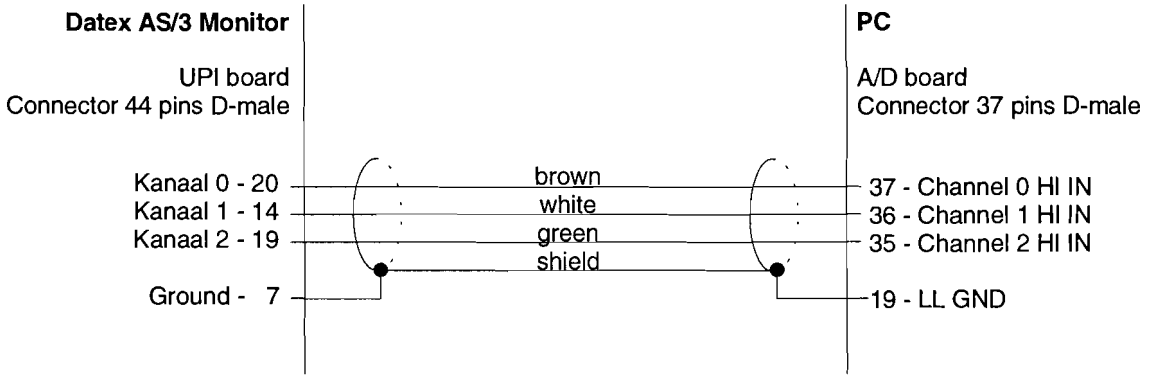

Link from Datex Relaxograph NMT-100
to PC with Keithley DAS-1402 A/D conversion board

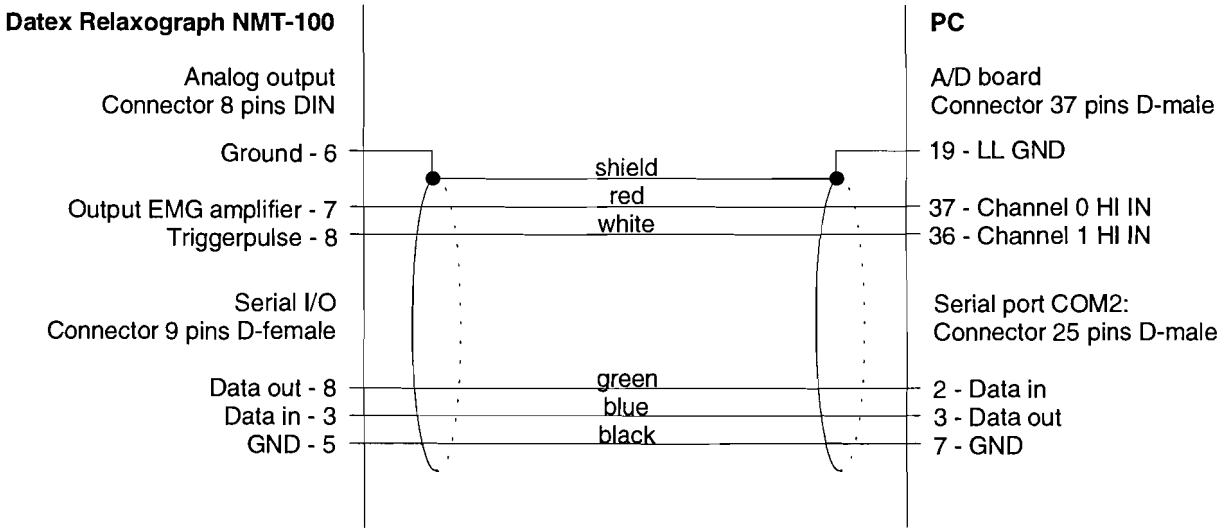

Appendix B - Validation parameters and their bounds

The TOF signal parameters that were used for validation of the learning and test sets are shown here. For the test set, all amplitude related criteria (with dimension V or Vs), were divided by 2, to adapt to the AS/3 ADU's output voltage range.

Table B.1 - Criteria for valid measurements. When two criteria are present, measurements are considered valid only if both are met.

Parameter applies to:	Parameter	Criterium 1	Criterium 2
Each ECAP in the TOF:	T_1	> 0 Vs	< 0.03 Vs
	T_2	> 0 Vs	< 0.03 Vs
	T_3	> 0 Vs	< 0.03 Vs
	T_4	> 0 Vs	< 0.03 Vs
	$V_{DC1,1}$	> -0.4 V	< 0.4 V
	$V_{DC1,2}$	> -0.4 V	< 0.4 V
	$V_{DC1,3}$	< 0.4 V	
	$V_{DC1,4}$	< 0.4 V	
	$V_{DC2,1}$	< 0.4 V	
	$V_{DC2,2}$	< 0.4 V	
	$V_{DC2,3}$	< 0.4 V	
	$V_{DC2,4}$	> -0.3 V	< 0.3 V
	$V_{DC3,1}$	> -0.3 V	< 0.2 V
	$V_{DC3,2}$	> -0.3 V	< 0.3 V
	$V_{DC3,3}$	> -0.3 V	< 0.3 V
	$V_{DC3,4}$	> -0.3 V	< 0.3 V
	$(V_{DC}/V_{PP})_1$	< -1.5	> 1.5
	$(V_{MAX}/T)_1$	> 25 s^{-1}	< 300 s^{-1}
	$(V_{MAX}/T)_2$	> 25 s^{-1}	< 300 s^{-1}
	$(V_{MAX}/T)_3$	> 25 s^{-1}	< 300 s^{-1}
	$(V_{MAX}/T)_4$	> 25 s^{-1}	< 300 s^{-1}
	$(V_{MIN}/T)_1$	< 36 s^{-1}	
	$(V_{MIN}/T)_2$	< 36 s^{-1}	
	$(V_{MIN}/T)_3$	< 36 s^{-1}	
	$(V_{MIN}/T)_4$	< 36 s^{-1}	
	$(V_{PP}/T)_1$	< 500 s^{-1}	
	$(V_{PP}/T)_2$	< 500 s^{-1}	
	$(V_{PP}/T)_3$	< 500 s^{-1}	
	$(V_{PP}/T)_4$	< 500 s^{-1}	
	$C_{irr,1}$	> 1.9	< 7
	$C_{irr,2}$	> 1.9	< 7
	$C_{irr,3}$	> 1.9	< 7
	$C_{irr,4}$	> 1.9	< 7
	$N_{0,1}$	< 6	
	$N_{0,2}$	< 7	
	$N_{0,3}$	< 7	
	$N_{0,4}$	< 7	

(continued)

Parameter applies to:	Parameter	Criterium 1	Criterium 2
Two ECAPs of the same TOF:	$NO_2 - NO_1$	> -5	< 5
	$NO_3 - NO_2$	> -5	< 5
	$NO_4 - NO_1$	> -5	< 5
	$NO_4 - NO_3$	> -5	< 5
	$T_2 - T_1$	< 0.005	
	$T_3 - T_2$	< 0.005	
	$T_4 - T_3$	> -0.01	< 0.01
	$T_4 - T_1$	< 0.005	
	$C_{irr,2} - C_{irr,1}$	> -1.8	< 1.8
	$C_{irr,3} - C_{irr,2}$	> -2.2	< 3
	$C_{irr,4} - C_{irr,3}$	> -2	< 2
Each TOF, compared to the last valid TOF:	$\Delta C_{irr,1}$	> -5	< 5
	$\Delta C_{irr,2}$	> -5	< 5
	ΔT_1	> -0.018 Vs	< 0.015 Vs
	ΔT_2	> -0.02 Vs	< 0.01 Vs
	ΔT_3	> -0.02 Vs	< 0.02 Vs
	ΔT_4	> -0.01 Vs	< 0.01 Vs
	$\Delta V_{DC1,1}$	> -0.4 V	< 0.4 V
	$\Delta V_{DC1,2}$	> -0.4 V	< 0.4 V
	$\Delta V_{DC1,3}$	< 0.4 V	
	$\Delta V_{DC1,4}$	< 0.4 V	
	$\Delta V_{DC2,1}$	< 0.4 V	
	$\Delta V_{DC2,2}$	< 0.4 V	
	$\Delta V_{DC2,3}$	< 0.4 V	
	$\Delta V_{DC2,4}$	> -0.3 V	< 0.3 V
	$\Delta V_{DC3,1}$	> -0.3 V	< 0.2 V
	$\Delta V_{DC3,2}$	> -0.3 V	< 0.3 V
	$\Delta V_{DC3,3}$	> -0.3 V	< 0.3 V
	$\Delta V_{DC3,4}$	> -0.3 V	< 0.3 V
	$\Delta(V_{MAX}/T)_1$	> -200 s^{-1}	< 200 s^{-1}
	$\Delta(V_{MAX}/T)_2$	> -200 s^{-1}	< 200 s^{-1}
	$\Delta(V_{MAX}/T)_3$	> -200 s^{-1}	< 200 s^{-1}
	$\Delta(V_{MAX}/T)_4$	> -200 s^{-1}	< 200 s^{-1}
	$\Delta V_{PP,1}$	> -5 V	
	$\Delta V_{PP,2}$	> -4 V	< 4 V
	$\Delta V_{PP,3}$	> -4 V	< 4 V
	$\Delta V_{PP,4}$	> -4 V	< 4 V
	$\Delta(V_{PP}/T)_1$	> -300 s^{-1}	< 300 s^{-1}
	$\Delta(V_{PP}/T)_2$	< 300 s^{-1}	
	$\Delta(V_{PP}/T)_3$	< 200 s^{-1}	
	$\Delta(V_{PP}/T)_4$	> -300 s^{-1}	< 300 s^{-1}